FLAVIN AMINE OXIDASES FROM THE MONOAMINE OXIDASE STRUCTURAL FAMILY UTILIZE A HYDRIDE TRANSFER MECHANISM

A Dissertation

by

MICHELLE HENDERSON POZZI

Submitted to the Office of Graduate Studies of
Texas A&M University
in partial fulfillment of the requirements for the degree of

DOCTOR OF PHILOSOPHY

May 2010

Major Subject: Biochemistry

FLAVIN AMINE OXIDASES FROM THE MONOAMINE OXIDASE STRUCTURAL FAMILY UTILIZE A HYDRIDE TRANSFER MECHANISM

A Dissertation

by

MICHELLE HENDERSON POZZI

Submitted to the Office of Graduate Studies of
Texas A&M University
in partial fulfillment of the requirements for the degree of

DOCTOR OF PHILOSOPHY

Approved by:

Co-Chairs of Committee,	Paul F. Fitzpatrick
	Gregory D. Reinhart
Committee Members,	Mary Bryk
	Frank M. Raushel
Head of Department,	Gregory D. Reinhart

May 2010

Major Subject: Biochemistry

ABSTRACT

Flavin Amine Oxidases from the Monoamine Oxidase Structural Family Utilize a Hydride Transfer Mechanism. (May 2010)

Michelle Henderson Pozzi, B.S., Sam Houston State University

Co-Chairs of Advisory Committee: Dr. Paul F. Fitzpatrick
Dr. Gregory D. Reinhart

The amine oxidase family of enzymes has been the center of numerous mechanistic studies because of the medical relevance of the reactions they catalyze. This study describes transient and steady-state kinetic analyses of two flavin amine oxidases, mouse polyamine oxidase (PAO) and human lysine specific demethylase (LSD1), to determine the mechanisms of amine oxidation.

PAO is a flavin adenine dinucleotide (FAD)-dependent enzyme that catalyzes the oxidation of N1-acetylated polyamines. The pH-dependence of the k_{cat}/K_{amine} indicates that the monoprotonated form of the substrate is required for catalysis, with the N4 nitrogen next to the site of CH bond cleavage being unprotonated. Stopped-flow spectroscopy shows that the pH-dependence of the rate constant for flavin reduction, k_{red}, displays a pK_a of 7.3 with a decrease in activity at acidic pH. This is consistent with an uncharged nitrogen being required for catalysis. Mutating Lys315 to methionine has no effect on the k_{cat}/K_{amine}-pH profile with the substrate spermine, and the k_{red} value only shows a 1.5-fold decrease with respect to wild-type PAO. The mutation results in a 30-fold decrease in k_{cat}/K_{O2}. Solvent isotope effects and proton inventories are consistent

with Lys315 accepting a proton from a water molecule hydrogen-bonded to the flavin N5 during flavin oxidation.

Steady-state and transient kinetic studies of *para*-substituted N,N'-dibenzyl-1,4-diaminobutanes as substrates for PAO show that the k_{red} values for each correlate with the van der Waals volume (V_W) and the σ value. The coefficient for V_W is the same at pH 8.6 and 6.6, whereas the ρ value increases from -0.59 at pH 8.6 to -0.09 at pH 6.6. These results are most consistent with a hydride transfer mechanism.

The kinetics of oxidation of a peptide substrate by human lysine specific demethylase (LSD1) were also studied. The k_{cat}/K_M pH-profile is bell-shaped, indicating the need for one unprotonated nitrogen next to the site of CH bond cleavage and another protonated nitrogen. The k_{cat} and k_{red} values are equal, and identical isotope effects are observed on $k_{red,}$ k_{cat}, and k_{cat}/K_M, indicating that CH bond cleavage is rate-limiting with this substrate.

DEDICATION

This dissertation is dedicated to my family. For my parents and grandmother, who have taught me through their words and actions how to live this life as stated in Philippians 3:14, “I press on toward the goal for the prize of the upward call of God in Christ Jesus.” To my husband for all the support, love, and friendship we share, strengthened by our faith and values to recognize true achievements in life, “Let not a wise man boast of his wisdom, and let not the mighty man boast of his might, let not a rich man boast of his riches; but let him who boasts boast of this, that he understands and knows Me” (Jeremiah 9:23-24). To my son, the highlight of my life, the greatest blessing and responsibility I have ever been given, and the one I want to give all opportunities. And finally to my precious little dogs who faithfully wait for my return from work every day and sit with me during long nights of study.

ACKNOWLEDGEMENTS

I would like to thank my advisor Dr. Paul F. Fitzpatrick for his expertise, guidance and support, and my committee members for their involvement in overseeing my progress throughout my graduate career. I would like to thank all of my lab mates who have been great co-workers and great friends. I would like to thank the many friends I have made in graduate school, who have made the bad times better and the good times great. And finally, I would like to thank my family for their unwavering support, encouragement, love, and most importantly, their prayers.

ABBREVIATIONS

DAAO	D-Amino acid oxidase
FAD	Flavin adenine dinucleotide
FMN	Flavin mononucleotide
Fms1	*S. cerevisiae* spermine oxidase
LAAO	L-Amino acid oxidase
LSD1	Lysine-specific demethylase 1
MAO	Monoamine oxidase
MTOX	*N*-Methyltryptophan oxidase
PAO	Polyamine oxidase
SSAT	Spermidine/spermine N1-acetyltransferase
TMO	Tryptophan 2-monooxygenase

TABLE OF CONTENTS

LIST OF FIGURES

FIGURE Page

LIST OF TABLES

CHAPTER I

INTRODUCTION

POLYAMINE METABOLISM AND REGULATION

Polyamines were originally isolated as "three-sided" crystals from human semen in 1678 by Antonie van Leeuwenhook (*1*), though the empirical formula of the crystals was not deduced until 1924 (*2*). Polyamines include N,N'-bis(3-amino-propyl)butane-1,4-diamine and N-(3-aminopropyl)butane-1,4-diamine, commonly referred to as spermine and spermidine for the source of their discovery, and 1,4-diaminobutane, which derives its common name of putrescine from its offensive smell that is associated with putrefying flesh. Oftentimes polyamines are referred to as supercations due to the multiple positive charges carried on nitrogens within the aliphatic chain. Polyamines, specifically spermine and spermidine, have been shown to interact with DNA, bridging the major and minor grooves (*3*). Structural studies indicate that these "bridging interactions" occur within an individual DNA molecule (*4*), and that polyamines selectively bind pyrimidine residues (*5*). Polyamine interactions have been suggested to not only alter DNA structure, but also influence its function (*6*). For example, in the nucleosome, the concentration of polyamines has been correlated with partial unwinding of DNA resulting in exposure of potential transcriptional regulators binding sites (*7*).

This dissertation follows the style of *Biochemistry*.

Though the positive charge associated with polyamines is a defining characteristic, polyamines in a cell vary in length, number of potential positive charges, flexibility and acetylation, indicating that cells requires multiple polyamines for differing functions. Polyamines include spermine, spermidine, their acetylated derivatives, and putrescine (Figure 1.1). Polyamine metabolism is a complex system that orchestrates biosynthesis, degradation and transport (Figure 1.2, modified from Ref (*8*)). In eukaryotic cells, the three polyamines spermine, spermidine and putrescine are synthesized from L-arginine and L-methionine. Putrescine is synthesized from L-arginine via arginase and ornithine decarboxylase. Putrescine can be converted into spermidine and spermine by spermidine synthase and spermine synthase, respectively, using an aminopropyl group from decarboxylated *S*-adenosylmethionine. The aminopropyl group is generated from L-methionine in two consecutive reactions involving methionine adenosyltransferase and *S*-adenosylmethionine decarboxylase.

Polyamine degradation begins with spermidine/spermine N1-acetyltransferase (SSAT) using acetyl-CoA to acetylate spermine and spermidine, producing N1-acetylspermine and N1-acetylspermidine. Polyamine oxidase (PAO) oxidizes N1-acetylspermine and N1-acetylspermidine to spermidine and putrescine, producing 3-acetamidopropanal and H_2O_2 as byproducts. More recently, it was determined that an enzyme catalyzes the back-conversion of spermine to produce spermidine, 3-aminopropanal, and H_2O_2. This enzyme has been named spermine oxidase to distinguish it from the aforementioned PAO.

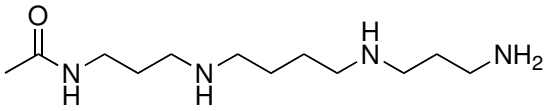

N1-acetylspermine

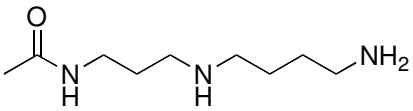

N1-acetylspermidine

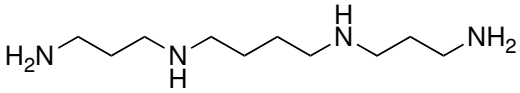

Spermine

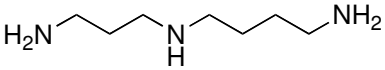

Spermidine

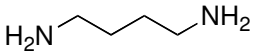

Putrescine

Figure 1.1: Polyamine structures.

Transport of polyamines into and out of the cell is part of polyamine homeostasis, though in mammalian cells the major production of polyamines occurs via biosynthesis (*9*). To date, a mammalian polyamine transporter has yet to be identified. Transport of polyamines in mammalian cells has been proposed to occur through two different models. The first involves transport of polyamines sequestered in vesicles into cells through unidentified transporters that operate via membrane potential (*10*). A second transport mechanism involves the uptake of spermine via heparin sulfate chains of glypican-1 (*11*). Polyamines are exported from the cell in a manner that is dependent on the cell's growth status; export of polyamines is increased when cell growth is halted and decreased when cells growth occurs (*12*).

The N1-acetylated polyamines are not found in normal cells because they are the main polyamines exported from the cell (*13*); however, higher concentrations are present in cancer cells indicating a direct link between changes in polyamine metabolism and carcinogenesis (*14, 15*). Furthermore, stoichiometric amounts of 3-acetamidopropanal and H_2O_2 produced during oxidation of acetylated polyamines have been shown to be involved in apoptosis (*16, 17*). The correlation with changes in polyamine metabolism and deviations from normal cell growth provide the opportunity for therapeutic intervention (*18*). Both ornithine decarboxylase and *S*-adenosylmethionine decarboxylase have been used as targets for inhibition, but in both instances inhibition has resulted in depletion of only two of the three polyamines (*19, 20*). In addition,

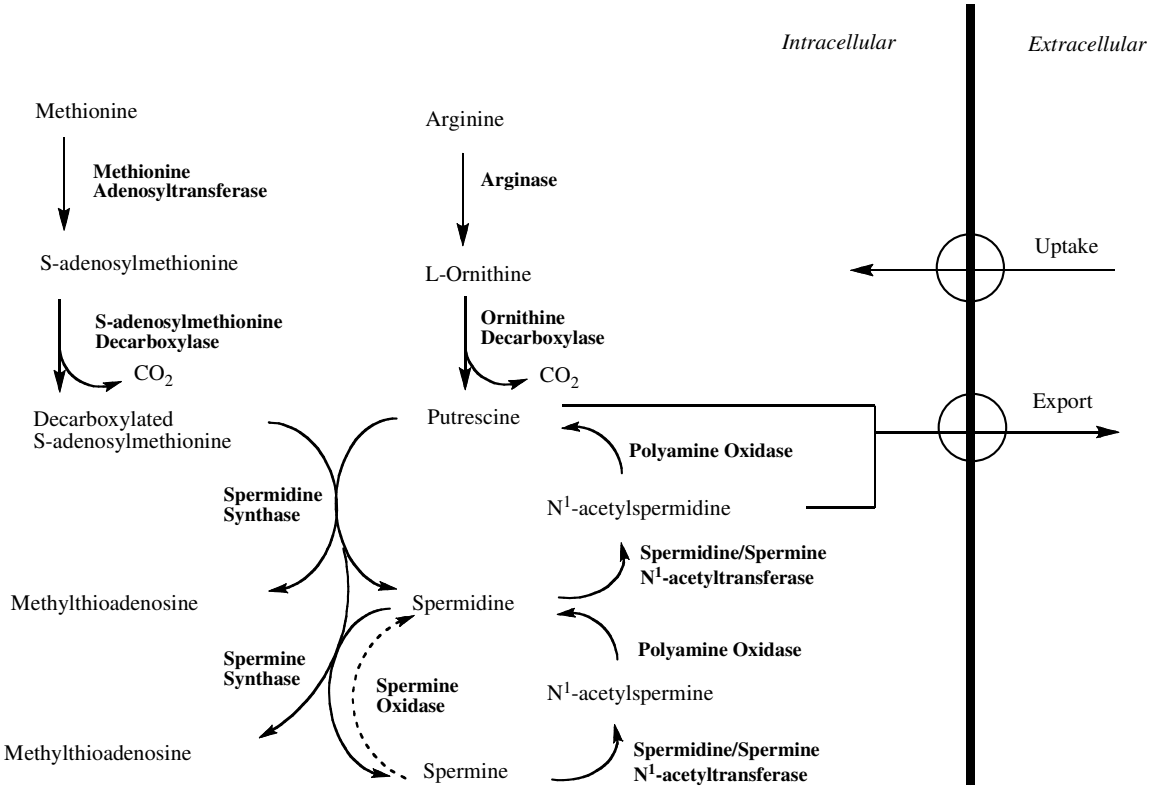

Figure 1.2: Polyamine metabolism.

both of these enzymes have rapid turnover in mammalian cells (*21*), making long term inhibition difficult. Since therapeutically the goal is to deplete polyamine levels within a cell, SSAT and PAO, which play a direct role in the catabolism of polyamines, are receiving greater attention in drug design. To date, an inhibitor specific for SSAT has not been developed, though it has been shown that inhibitors of other enzymes in polyamine metabolism induce SSAT activity also (*22*). Inhibitors of PAO have shown to be promising, with a number of clinical trials underway (*23, 24*). Studies using a lung carcinoma cell line suggest that induction of PAO results in increased production of H_2O_2 linked with cytotoxicity and eventual apoptosis (*25*). These results taken cumulatively show the potential for the use of polyamine analogues as chemopreventative and anticancer drugs, necessitating the need to better understand the mechanisms of each of the enzymes involved in polyamine metabolism.

POLYAMINE OXIDASE

PAO contains a non-covalently bound flavin adenine dinucleotide (FAD) and is one of two enzymes that are involved in polyamine catabolism as previously described. Despite PAO having been implicated in cancer, ischemic tissue damage and apoptosis, little attention has been paid to the mechanism of this enzyme, necessitating the need to do so. The cloning, sequencing and expression of mouse PAO (*26*) presents the opportunity to study a mammalian PAO in an effort to gain important mechanistic information that can be used for better and more efficient drug design.

Mammalian PAOs are differentiated from plant PAOs based on the site of CH bond cleavage. In a mammalian PAO, N1-acetylated polyamines are oxidized on the *exo*-side of their N4-amino groups (Figure 1.3) producing an imine-intermediate that is non-enzymatically hydrolyzed. 3-Acetamidopropanal is formed, which can be enzymatically deacetylated to produce cytotoxic 3-aminopropanal (*27*). Mouse PAO exhibits a preference for polyamine substrates in the order N1-acetyl spermine ≈ N1-acetyl spermidine >> N1,N12-diacetyl spermine >> spermine (*28*). With plant PAOs, the carbon on the *endo*-side of the N4-nitrogens of spermidine and spermine is oxidized, producing 4-aminobutyraldehyde and 3-(aminopropyl)-4-aminobutyraldehyde, respectively.

The difference in substrate specificity of enzymes involved in polyamine metabolism raises questions about nomenclature to differentiate between such enzymes. Specifically, PAO's preference for N1-acetylated polyamines distinguishes it from an amine oxidase that catalyzes the oxidation of spermine, more accurately defining the latter as a spermine oxidase. From this perspective, it could be argued that the preference for plant PAO`s to oxidize spermine and spermidine over their acetylated derivatives would more accurately classify these enzymes as being spermine oxidases.

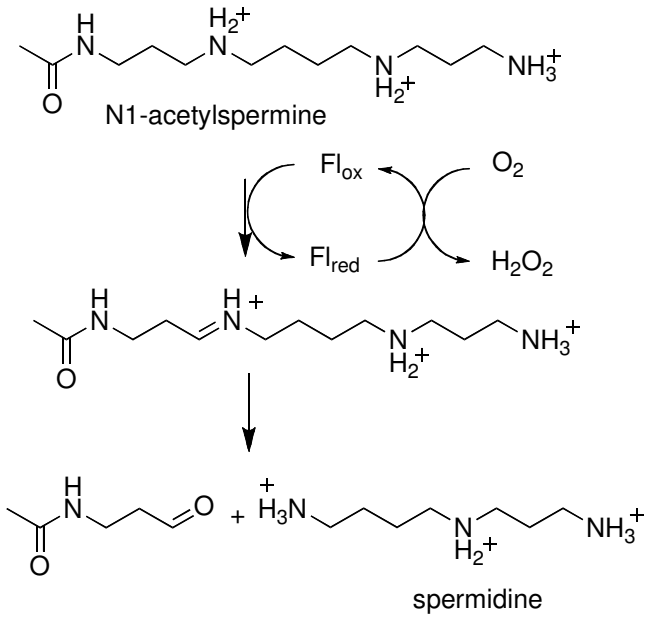

Figure 1.3: PAO oxidation of N1-acetylspermine.

FLAVOPROTEIN AMINE OXIDASES

PAO is a member of a family of enzymes known as flavin amine oxidases. The overall reaction of these enzymes can be divided into two half-reactions (Figure 1.4). The reductive half-reaction is characterized by the reduction of the flavin cofactor upon the oxidation of substrate. The oxidative half-reaction involves the oxidation of enzyme with reduced FAD by molecular oxygen, producing H_2O_2 and an imine intermediate that is non-enzymatically hydrolyzed.

The flavin cofactor exists in three forms. The first form is riboflavin (vitamin B_2), which can be converted to the other two forms flavin mononucleotide (FMN) and flavin adenine dinucleotide (FAD) as shown in Figure 1.5 (modified from ref (*29*)). Flavins possess a highly conjugated ring system that gives them a chemical reactivity that allows them to accept one electron, forming flavin semiquinone, or two electrons to form reduced flavin (Figure 1.6, modified from ref (*29*)). Figure 1.7 shows representative UV-visible absorbance spectra for the oxidized, semiquinone, and reduced states of flavin, with indicated wavelengths of maximum absorbance in each state (*30*). Flavin oxidation potentials are in the range of 0 to -200 mV, though -500 mV has been observed in flavodoxins (*29*). Flavins can be non-covalently bound in flavoenzymes, as is the case with PAO (*26*), or covalently bound as with MAO, which occurs via a thioether linkages between a cysteinyl residue and the 8α-methylene of the isoalloxazine ring (*31*).

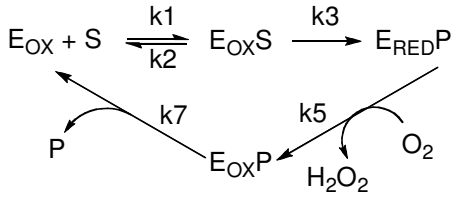

Figure 1.4: General reaction mechanism for flavoprotein amine oxidases.

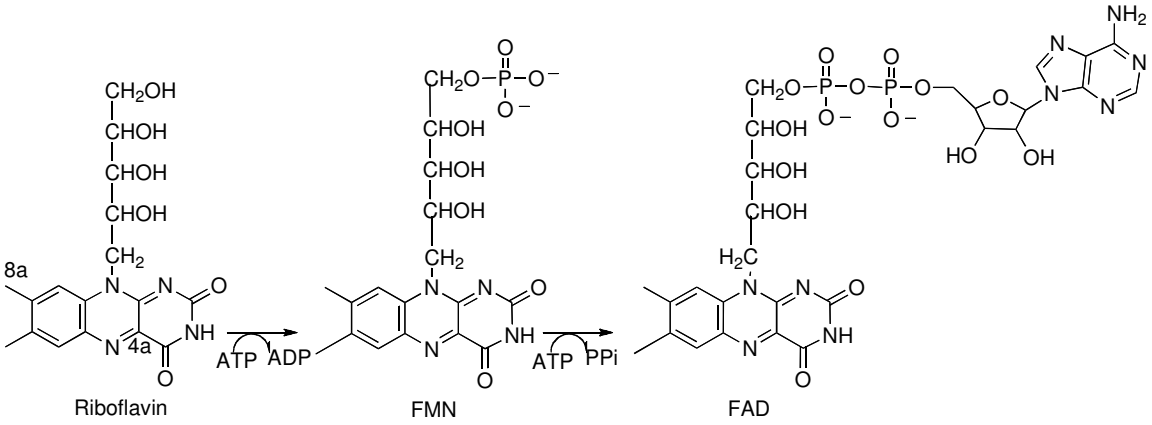

Figure 1.5: Conversion of riboflavin to FMN and FAD.

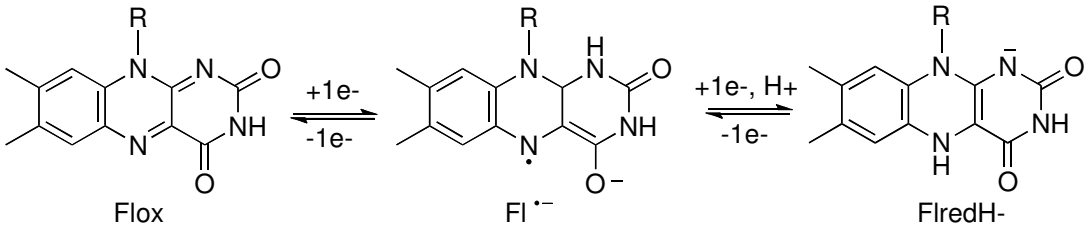

Figure 1.6: Electronic conversion of oxidized flavin to semiquinone to reduced flavin.

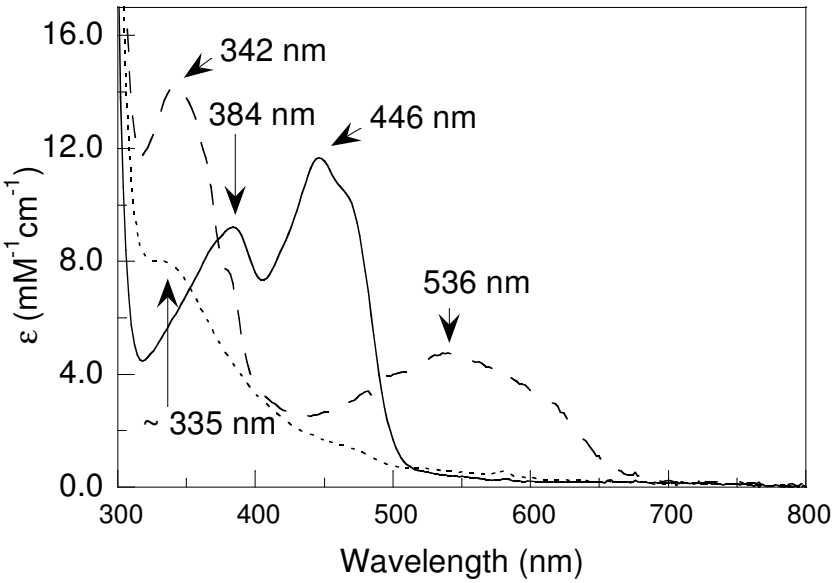

Figure 1.7: UV-visible spectra of oxidized flavin (solid line), semiquinone (dotted line), and reduced flavin (dashed line).

PAO belongs to the MAO structural family, which is distinguished by an easily identifiable N-terminal βαβ FAD-binding motif that interacts with the ADP portion of the FAD cofactor and a second conserved region in the C-terminus involved in FAD binding (*26*). In addition to MAO and PAO, other members of this family include the newly discovered human lysine-specific demethylase-1 (LSD1) involved in epigenetic regulation (*32*), Fms1, a yeast spermine oxidase (*33*), L-amino acid oxidase (*34*), and tryptophan 2-monooxygenase (*35*).

The mechanism of these flavoproteins has been the source of controversy and debate. MAO A and B, which catalyze the oxidation of amine neurotransmitters, have been the center of intense study for years due to their important role in medical treatment. MAO A has been linked to depression arising from decreases of norepinephrine and serotonin levels in the brain (*36*), and MAO B has been shown to involved in the degeneration associated with Parkinson's disease (*37*). To date, three prominent mechanisms for substrate oxidation by this family of enzymes exist, a single electron transfer (SET) mechanism, a polar nucleophilic mechanism, and a hydride transfer mechanism.

The SET mechanism, as shown in Fig 1.8 (adapted from ref (*38*)), is initiated by a single electron transfer from the substrate amine to the covalently bound flavin, producing a substrate aminium radical cation and a flavin semiquinone as transient intermediates. The lowered pK_a of the α-CH bond of the aminium radical cation can result in proton loss and a second electron transfer to the flavin semiquinone producing reduced flavin or can go through a radical recombination to give a covalent adduct that can undergo β-elimination to produce the iminium ion. This mechanism was proposed based on studies using amine analogues containing cyclopropyl substituents as reporters (*39*). Silverman took results of kinetic and spectroscopic studies of MAO with these mechanism-based inactivators as evidence for the formation of an amine radical cation and flavin semiquinone in the normal catalytic mechanism. The SET mechanism has some potential flaws, including a lack of spectral data showing an intermediate flavin semiquinone or active site radical and the requirement for a flavin potential of approximately 1.5 V for the proposed one electron oxidation of primary amines (*40*). Further, the inactivation of methonal oxidase by cyclopropyl alcohol (*41*) and cholesterol oxidase with 2α,3α-cyclopropano-5α-cholestan-3β-ol (*42*) have been explained to occur through mechanisms not involving radical intermediates.

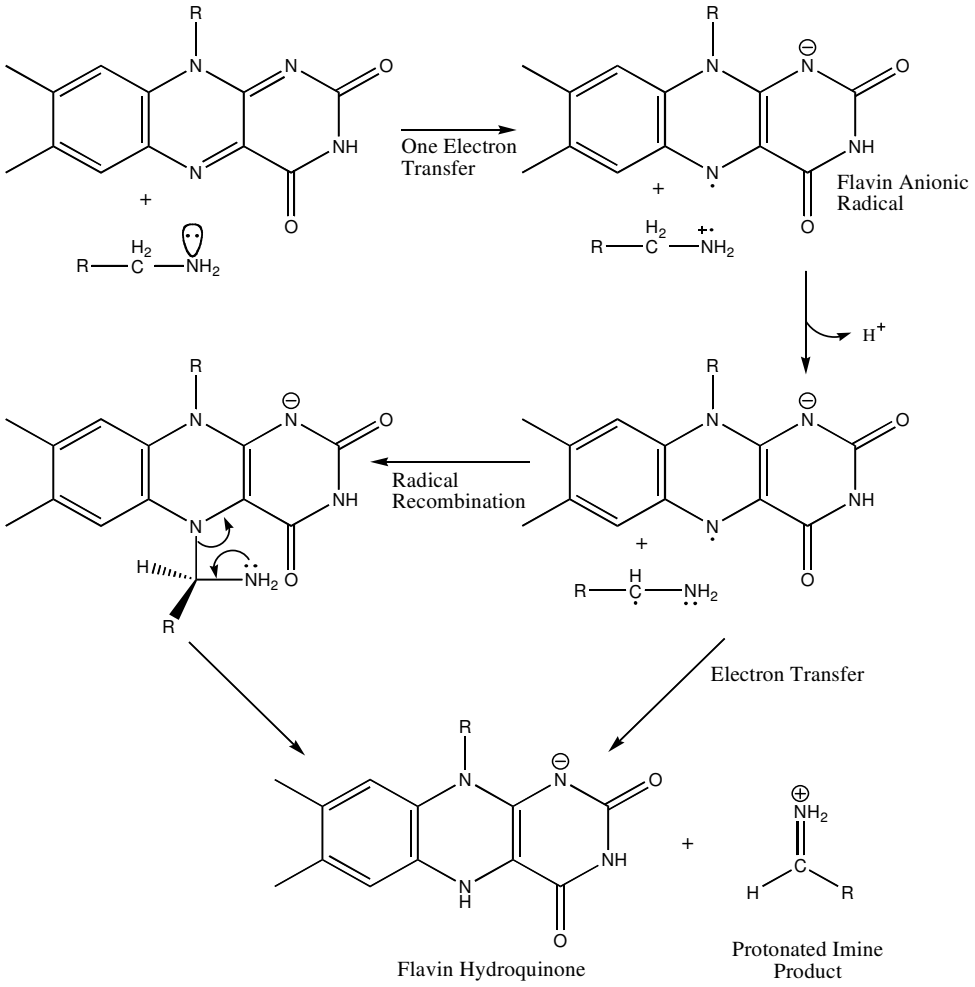

Figure 1.8: The SET mechanism.

The polar nucleophilic mechanism shown in Figure 1.9 (adapted from ref (*38*)) involves the covalent attachment of the substrate amine to the C4a-position of the flavin, activating the N5-position for proton abstraction of the α-hydrogen. This mechanism was originally proposed by Hamilton (*43*), but has been supported by Edmondson (*44*). The evidence for this mechanism comes from quantitative structure-activity relationship studies of MAO A with a series of para-substituted benzylamine analogues in which Miller and Edmondson report a positive correlation of the rate constant for flavin reduction with the electronic parameter σ and a ρ value of 1.8 ± 0.3 (*45*). The sign and magnitude of this ρ value is indicative of reactions that are aided by electron-withdrawing substituents. However, these results are not consistent with previous observations with substituted benzylamines as substrates for MAO B, where correlation between the rate constant for flavin reduction and the Taft steric parameter indicates that sterics are more important for flavin reduction (*46*). The reason for the difference in the ρ value for MAO-A versus MAO-B is unclear, especially since MAO-A and MAO-B are 70% identical.

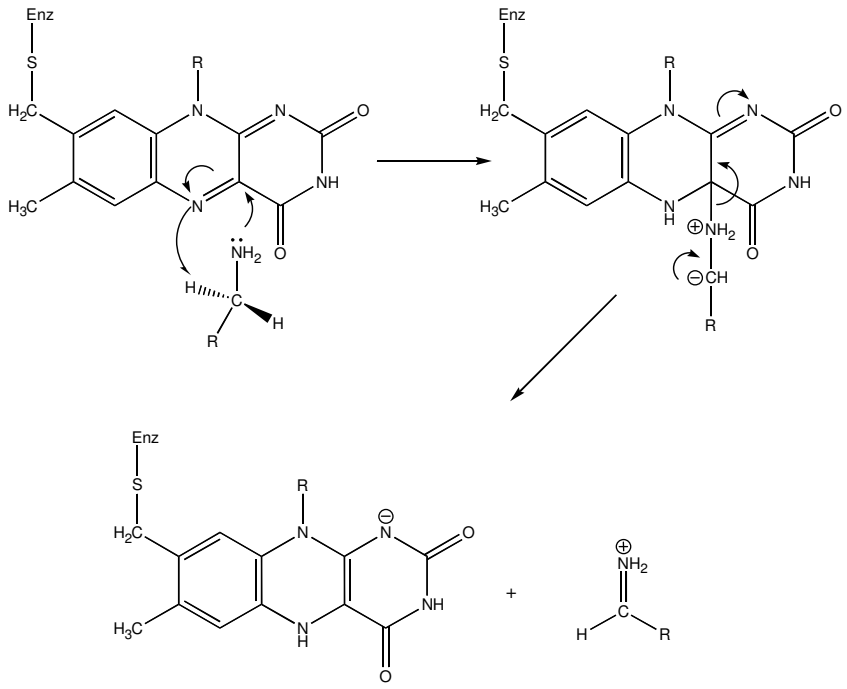

Figure 1.9: The polar nucleophilic mechanism.

The hydride transfer mechanism is the generally accepted mechanism of the flavoprotein amine oxidase D-amino acid oxidase (DAAO), which has a different structure than the MAO structural family. This mechanism, as shown in Figure 1.10, involves the direct transfer of a hydride equivalent from the substrate to the flavin cofactor with no intermediate steps. This mechanism has received greater attention in recent years as the mechanism of flavoprotein amine oxidases in light of new kinetic data. Deuterium and ^{15}N kinetic isotope effect studies of flavin amine oxidases, including DAAO (*47, 48*), tryptophan-2-monooxygenase (TMO) (*49*), and *N*-methyltryptophan oxidase (MTOX) (*50, 51*), are most consistent with a hydride transfer mechanism. Furthermore, these results indicate that a common kinetic mechanism is shared between the DAAO structural family, which includes DAAO (*52*) and MTOX (*50*), and the MAO structural family that includes TMO (*53*).

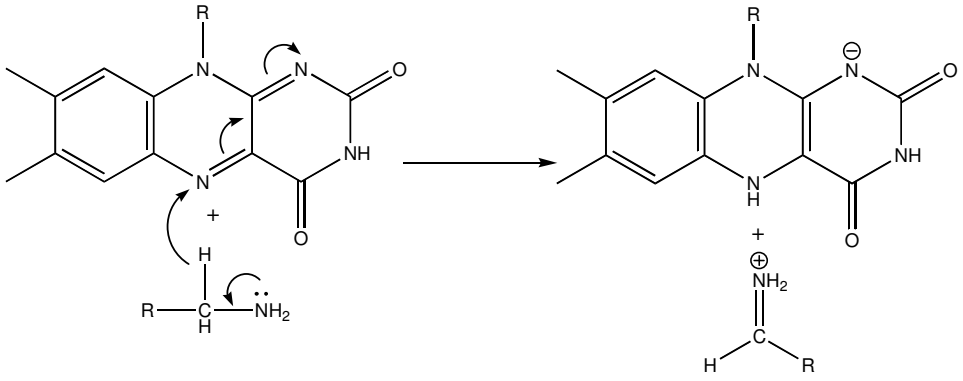

Figure 1.10: The hydride transfer mechanism.

PAO presents the opportunity to study a flavin amine oxidase in an effort to determine the chemical mechanism, assess the potential importance of residues within the active site, and to gain insight into substrate specificity. Results of this study with a mammalian PAO can serve to offer structural and mechanistic information that can be utilized in drug design for anti-cancer agents targeted for PAO.

CHAPTER II

pH DEPENDENCE OF A MAMMALIAN POLYAMINE OXIDASE: INSIGHTS INTO SUBSTRATE SPECIFICITY AND THE ROLE OF LYSINE 315*

The polyamines spermine and spermidine are essential for cell proliferation, with higher levels being found in rapidly growing cells (*4, 54*). This observation suggests that compounds which decrease the levels of polyamines in cells have potential as antineoplastic agents. Indeed, the polyamine biosynthetic pathway has been heavily studied with the goal of developing enzyme inhibitors (*24, 54, 55*). The pathway begins with the formation of putrescine from ornithine catalyzed by ornithine decarboxylase. Putrescine is then converted to spermine by two sequential reactions catalyzed by spermidine synthase, forming first spermidine and then spermine, using decarboxylated S-adenosylmethionine as the propylamine donor in both steps. In the opposite direction, catabolism of spermine requires the sequential action of two enzymes (*4*). First, acetylation of spermine by spermidine/spermine N1-acetylspermine acetyltransferase forms N1-acetylspermine. This is then converted to spermidine by the flavoenzyme polyamine oxidase (PAO). The same two enzymes also catalyze the acetylation of spermidine to N1-acetylspermidine and the subsequent oxidation to putrescine. Very recently, several mammalian tissues have been found to contain a flavoenzyme capable of oxidizing spermine directly to spermidine (*56-58*); while referred to occasionally as PAO, it is more accurately a spermine oxidase.

The reaction of mammalian PAO is shown in Figure 1.3. The enzyme cleaves the *exo* carbon-hydrogen bond of its substrate, forming spermidine and N-acetyl-3-aminopropanaldehyde from N1-acetylspermine or putrescine and N-acetyl-3-aminopropanaldehyde from N1-acetylspermidine. There are also plant PAOs, of which the maize enzyme is the best-characterized (*59-62*). While the mammalian enzymes oxidize spermine to 3-aminopropanaldehyde and spermidine, the plant enzymes oxidize the *endo* bond of spermine to form propane-1,3-diamine and N-(3-aminopropyl)-4-aminobutyraldehyde (*63*). The structural bases for the difference in substrate specificity between polyamine and spermine oxidases and in the site of substrate oxidation between the plant and animal enzymes are not known.

The general reaction of flavin amine oxidases such as PAO can be divided into two half reactions. In the reductive half reaction a hydride equivalent is transferred from the substrate to the flavin, while the oxidative half reaction involves the oxidation of the reduced flavin by molecular oxygen, producing H_2O_2. The steady-state kinetic mechanism has previously been determined for mouse PAO (*26*). Consistent with the results for most flavoprotein oxidases (*64*), the kinetic pattern is ping-pong due to the reductive half reaction being effectively irreversible. Consequently, the k_{cat}/K_m value for the amine substrate includes the steps in the reductive half-reaction from amine binding through flavin reduction, while the k_{cat}/K_m value for oxygen is the second order rate constant for reoxidation of the reduced flavin. This simplifies analysis of the individual kinetic parameters, since the k_{cat}/K_m value for the amine substrate is independent of the

oxygen concentration, while the rate constant for flavin reduction can readily be determined using rapid-reaction methods in the absence of oxygen.

The chemical mechanism of the reductive half-reaction of flavoprotein amine oxidases has been quite controversial (*65*). Oxidation of an amine substrate by an amine oxidase necessarily involves the removal of two protons and two electrons as the carbon-nitrogen single bond is converted to a double bond. The various mechanistic proposals for the flavin amine oxidases have included most of the possible combinations by which this can occur (*65, 66*). Cleavage of the carbon-hydrogen bond could occur by removal of the hydrogen as a proton, a hydrogen atom, or a hydride (*44, 67, 68*), with some mechanisms involving formation of an amine-flavin adduct as an intermediate (*44*). In contrast, the hydrogen is generally proposed to be removed from the nitrogen as a proton, with the disagreement over when this occurs in the reaction. Thus, the proton could be lost to solvent before the amine binds to the protein (*48*) or to an active site base either before (*69-71*) or concurrent with cleavage of the carbon-hydrogen bond (*69*). Thus, establishing the catalytic mechanism of an amine oxidase necessarily requires knowledge of the timing of removal of hydrogens from both the carbon and the nitrogen. In addition, in the case of the proton on the nitrogen, loss of the proton from the bound substrate would require an active site base.

The flavin amine oxidases can be divided into two structural classes, the MAO/PAO family (*34, 60*) and the D-amino acid oxidase (DAAO)/sarcosine oxidase family (*72*). No structure of a mammalian PAO has been described to date. However, structures are available for maize PAO and for *S. cerevisiae* spermine oxidase (Fms1)

(*73, 74*). These enzymes both belong to the monoamine oxidase (MAO) family of flavoprotein amine oxidases (*73*). The sequences of mammalian PAOs align well with these and other members of this family (*26, 73, 75*). The available structures of members of the MAO family show that all contain a conserved lysyl residue in the active site (*32, 34, 73, 74, 76*). This residue is part of a "Lys-H_2O-N5" motif in which the lysyl side chain forms hydrogen bonds to the N5 of the isoalloxazine ring via an intervening water molecule. This lysyl residue has been proposed to be an active site base which accepts a proton from either the protonated amine of the substrate prior to its oxidation or from a water molecule to form hydroxide for hydrolysis of an imine intermediate (*34, 59*).

This chapter describes the use of the effects of pH on the steady-state and reductive half-reaction kinetics of mouse PAO to probe substrate specificity and establish the protonation states of polyamines required for catalysis. In addition, the role the conserved lysyl residue plays in amine oxidation by this enzyme has been analyzed.

EXPERIMENTAL PROCEDURES

Materials. Spermine was purchased from Acros Organics (Geel, Belgium), and 1,8-diaminooctane and 1,12-diaminododecane were purchased from Aldrich (Milwaukee, WI). N1-Acetylspermine and N1-acetylspermidine were synthesized as previously described (*77*); N1-acetylspermidine was also purchased from Fluka (Switzerland). Substrates were synthesized by Dr. Vijay Gawandi of Texas A&M University (*78*).

Expression and Purification of Recombinant Proteins. Mouse PAO was purified as previously described (*79*) with a few minor changes. The pellet resulting from the final 65% ammonium sulfate precipitation was resuspended in 50 mM potassium phosphate and 10% glycerol (pH 7.5) and dialyzed overnight with two buffer changes. The resulting protein sample was then centrifuged at 22,400xg for 30 min at 4 ºC to remove precipitated protein. The purified protein was stored at -80 ºC. The concentration of active enzyme was determined from the flavin visible absorbance spectrum, using an ε_{458} value of 10,400 M^{-1} cm^{-1}.

The K315M mutation was introduced using the Stratagene QuikChange site-directed mutagenesis method and the mutagenic primer 5'-GGCTTCGGTACCAACAAC**ATG**ATCTTCCTCGAGTTC -3', which contains the K315M mutation (shown in bold) and a silent mutation at Leu318 that results in the addition of an AvaI site (underlined) used in screening colonies. The DNA sequence of the entire gene was verified to ensure that no unwanted mutations occurred. Purification of the mutant enzyme was done using the same procedure as for wild type PAO.

Assays. Steady state kinetic assays were performed in air-saturated buffers on a computer-interfaced Hansatech (Hansatech Instruments) or YSI oxygen (Yellow Springs Instrument, Inc.) electrode. Assays were initiated by the addition of enzyme. All buffers contained 10% glycerol; 50 mM Tris-HCl, 50 mM CHES, and 50 mM CAPS were used for the pH ranges 7-8.5, 9.0-9.5, or 10-11 respectively.

Rapid-reaction kinetic experiments were conducted at 20 ºC on an Applied Photophysics SX-18MV stopped-flow spectrophotometer. The night before the experiment, the instrument was flushed with anaerobic buffer followed by a solution of 36 nM glucose oxidase in 5 mM glucose, 50 mM Tris-HCl, pH 7.5. For enzyme solutions, anaerobic conditions were established by applying cycles of vacuum and argon, while substrate solutions were bubbled with argon. All buffers contained 10% glycerol and 5 mM glucose; 200 mM PIPES, 200 mM Tris-HCl, and 200 mM CHES were used for the pH ranges 6.5-6.9, 7-8.9, or 9.0-9.5, respectively. Glucose oxidase was added to all anaerobic solutions at a final concentration of 36 nM before loading them onto the stopped-flow spectrophotometer.

Data Analysis. Kinetic data were analyzed using the programs KaleidaGraph (Adelbeck Software, Reading, PA) and Igor (WaveMetrics, Lake Oswego, OR). Initial rate data obtained by varying the concentration of a single substrate were fit to the Michaelis-Menten equation. The effects of pH on kinetic parameters were fit to equations 2.1-2.3. Equation 2.1 applies for a kinetic parameter which decreases below pK_1 due to the protonation of a single moiety. Equation 2.2 applies for a kinetic parameter which decreases above pK_2 due to the protonation of a single moiety.

Equation 2.3 applies for a kinetic parameter which decreases below pK_1 due to protonation of a single moiety and decreases above pK_2 due to deprotonation of a single moiety. In all three equations, c is the pH-independent value. In each, y is the kinetic parameter being measured, c is the pH-independent value, K_1 is the ionization constant for a residue which must be unprotonated, and K_2 is the ionization constant for a residue which must be protonated.

$$\log y = \log (c/(1 + H/K_1)) \quad (2.1)$$

$$\log y = \log (c/(1 + K_2/H)) \quad (2.2)$$

$$\log y = \log (c/(1 + H/K_1 + K_2/H)) \quad (2.3)$$

Analysis of stopped-flow data was done using both KaleidaGraph and SPECFIT (Spectrum Software Associates, Marlborough, MA). To determine the kinetic parameters for the reduction of wild type PAO by N1-acetylspermine, stopped-flow traces were fit to equation 2.4, which describes a triphasic exponential decay, where k_1, k_2, and k_3 are first order rate constants, A_1, A_2, A_3 correspond to the absorbance changes in each phase, and A_∞ is the final absorbance. Equation 2.5 was used to fit the biphasic traces obtained for K315M PAO.

$$A_t = A_1e^{-k_1t} + A_2e^{-k_2t} + A_3e^{-k_3t} + A_\infty \quad (2.4)$$

$$A_t = A_1e^{-k_1t} + A_2e^{-k_2t} + A_\infty \quad (2.5)$$

RESULTS

k_{cat}/K_{amine}- pH Profile. Previous steady-state kinetic studies at pH 7.6 indicated that the substrate preference for mouse PAO is N1-acetylspermine, N1-acetylspermidine, and then spermine, with spermine being a significantly slower substrate than the acetylated compounds (*26*). The effect of pH on the kinetic parameter k_{cat}/K_{amine} was determined for each of these three substrates. The results are shown in Figure 2.1A, and the resulting pK_a values are summarized in Table 2.1. The pH profiles for all three substrates exhibit decreases in activity at both low and high pH, consistent with a requirement for one moiety in the enzyme or substrate that must be protonated for substrate recognition and/or oxidation and one which must be unprotonated. Both acetylated substrates have bell-shaped curves with two distinguishable pK_a values. In contrast, with spermine the pH profile exhibits a sharp optimum so that the two pK_a values are too close together to resolve; consequently, only the average of the two pK_a values could be determined with this substrate.

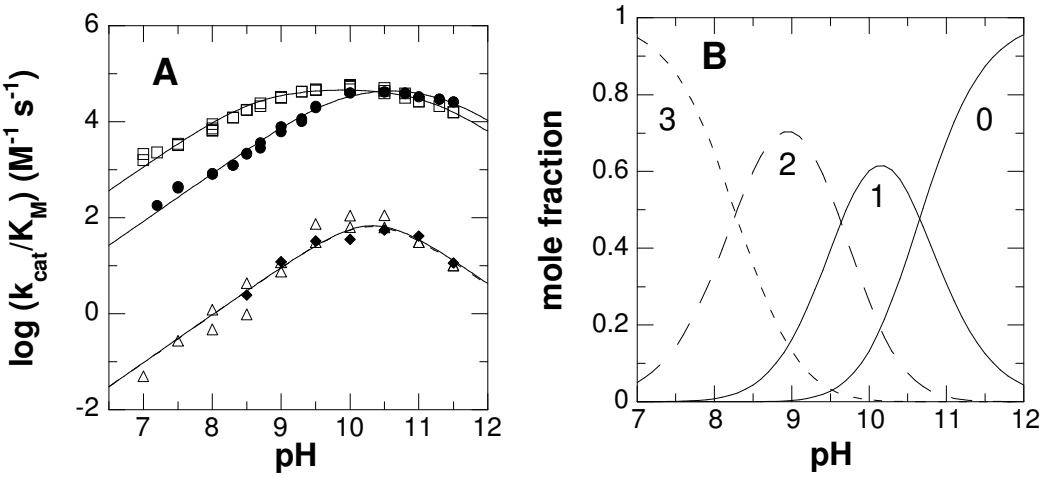

Figure 2.1: A, k_{cat}/K_{amine}-pH profile of wild type PAO with N1-acetylspermine (□), N1-acetylspermidine (●), and spermine (△), and K315M PAO (♦) with spermine. The lines are from fits of the data to eq 2.3. B, Theoretical protonation states of N1-acetylspermine with no proton, 1 proton, 2 protons, or 3 protons.

Table 2.1: pK_a values for PAO substrates and inhibitors

Kinetic parameter	**pKa_1**	**pKa_2**
Wild-type PAO		
k_{cat}/K_m for N1-acetylspermine	8.5 ± 0.1	11.2 ± 0.1
k_{cat}/K_m for N1-acetylspermidine	9.8 ± 0.1	11.3 ± 0.3
k_{cat}/K_m for spermine	10.3 ± 0.1	10.3 ± 0.1
K_i for N1-acetyl-1,8-diaminooctane	-	11.6 ± 0.1
K_i for 1,8-diaminooctane	9.3 ± 0.1	10.8 ± 0.1
K_i for N1-acetyl-N3-pentyl-1,3-diaminopropane	8.9 ± 0.1	-
K_i for 1,12-diaminododecane	10.0 ± 0.1	10.0 ± 0.1
K_i for N1-acetyl-1,12-diaminododecane	-	11.6 ± 0.1
K315M PAO		
k_{cat}/K_m for spermine	10.3 ± 0.1	10.3 ± 0.1

Protonation States of Polyamines as a Function of pH. A likely basis for one or both of the pK_a values in the k_{cat}/K_{amine}-pH profiles is the protonation state of the substrates. Figure 2.1B shows the effect of pH on the mole fractions of N1-acetylspermine with zero, one, two, or three protons (*78*). The monoprotonated form is maximal at pH 10.1, in good agreement with the pH optimum in the k_{cat}/K_{amine}-pH profile of 9.9, while the diprotonated form is maximal at pH 9.0. For spermine the pH maximum for the monoprotonated form is 10.4-10.5 (*78, 80, 81*), similarly closer to the pH optima of 10.3 than is the maximum for the diprotonated form of 9.4-9.5. The agreement with N1-acetylspermidine is not as good, in that the optimum in the k_{cat}/K_{amine}-pH profile is 10.5 while the calculated maximum for the monoprotonated form is 9.9 (*78*). However, a requirement for the diprotonated form of N1-acetylspermidine would contribute a single pK_a of 9.1 for a group which must be protonated to the k_{cat}/K_{amine}-pH profile, while a requirement for the uncharged form would contribute a single pK_a value of 10.6 (*78*), in contrast to the observed bell-shaped profile. Thus, the k_{cat}/K_{amine}-pH profiles are most consistent with the active form of the substrate having a single charge.

PAO pH Dependence of Inhibition. While the k_{cat}/K_{amine}-pH profiles are consistent with the monoprotonated forms of the substrate being preferred, they do not establish which nitrogen in each substrate must be charged. In addition, the k_{cat}/K_{amine}-pH profiles reflect both binding and catalysis. To determine the preferred protonation states of individual nitrogens in substrates for productive binding, analogues lacking one or more nitrogens (Figure 2.2) were characterized as inhibitors. 1,8-Diaminooctane, N1-

acetyl-1,8-diaminooctane, and N1-acetyl-N3-pentyl-1,3-diaminopropane all mimic the substrate N1-acetylspermidine. Each is a competitive inhibitor versus the amine (data not shown). The pK_i-pH profile for 1,8-diaminooctane is bell-shaped with the tightest binding at pH 10 (Figure 2.3A, Table 2.1), consistent with binding requiring that one nitrogen on the inhibitor be protonated and one be unprotonated. With N1-acetyl-1,8-diaminooctane the only protonatable group is the amino group on carbon 8; in this case the pK_i-pH profile shows a decrease at high pH with a pK_a value of 11.6 ± 0.1, but no decrease at low pH (Figure 2.3A). This is most consistent with the acidic pK_a in the pH profile for N1-acetylspermine being due to a need for N9 to be charged. N1-Acetyl-N3-pentyl-1,3-diaminopropane also has only one protonatable nitrogen group, located at the 4 position, the site of oxidation in N1-acetylspermidine. In this case, the pK_i-pH profile shows a decrease at low pH with a pK_a value of 8.9 ± 0.1, but no decrease at high pH, indicating that the N4 nitrogen must be unprotonated. These results are consistent with the active form of N1-acetylspermidine being the monoprotonated species in which the N9 nitrogen is protonated and the N4 nitrogen is unprotonated.

Similar studies were conducted with analogues of N1-acetylspermine and spermine. 1,12-Diaminododecane shows a bell-shaped pK_i-pH profile with an average pK_a value of 10.0 ± 0.1 (Figure 2.3B). This matches well the k_{cat}/K_{amine}-pH profile for spermine (Table 2.1), consistent with productive binding requiring a substrate with a single positive charge. The pK_i-pH profile for the N1-acetylspermine analogue N1-acetyl-1,12-diaminododecane shows a decrease at high pH with a single pK_a value of

11.6 ± 0.1 (Figure 2.3B), confirming that a nitrogen not located next to the site of CH bond cleavage must be protonated for catalysis.

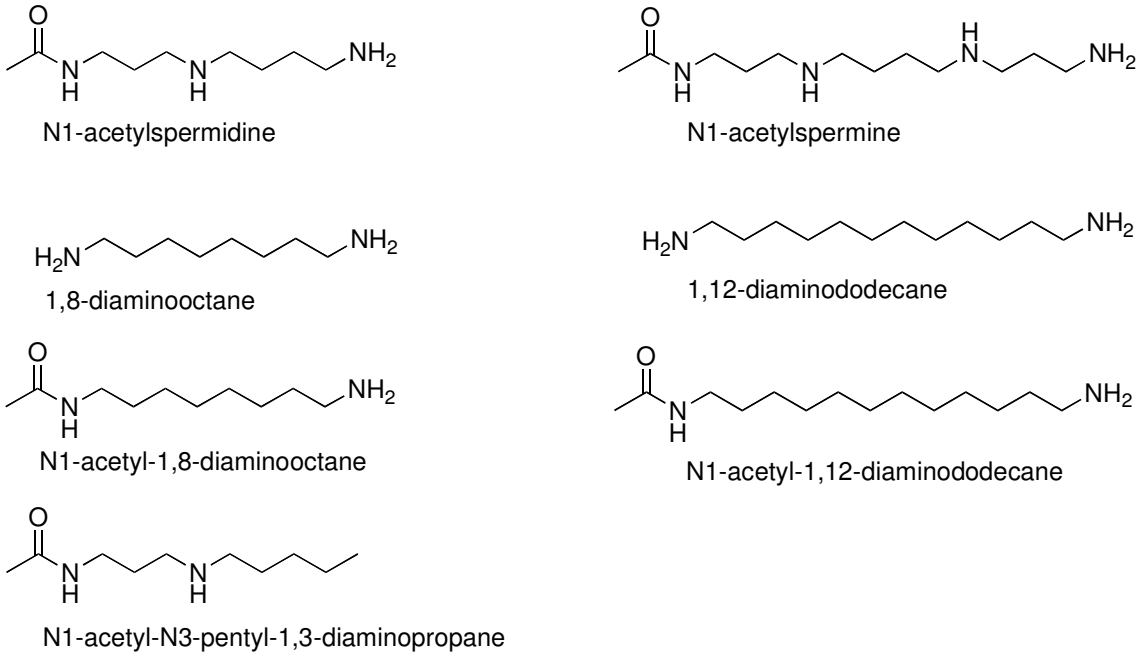

Figure 2.2: Structures of N1-acetylspermidine and N1-acetylspermidine analogues.

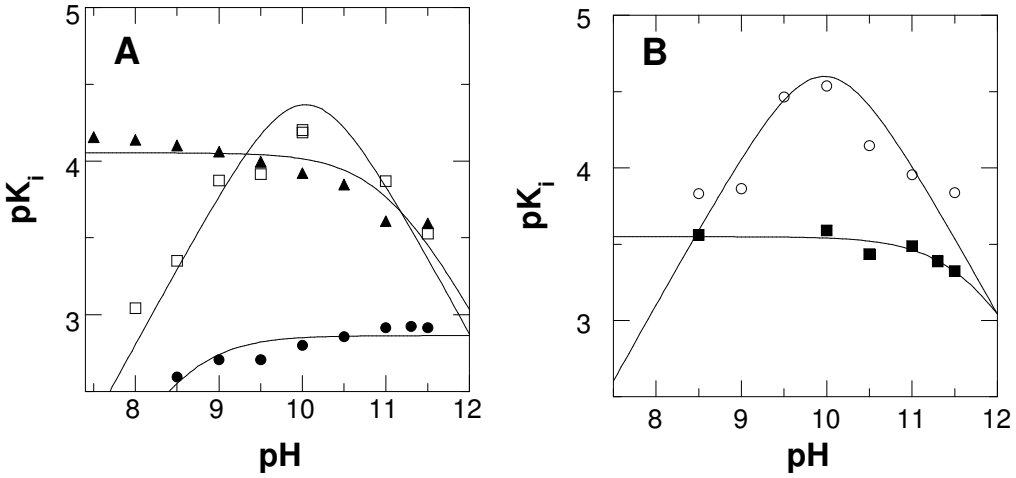

Figure 2.3: pK_i-pH profile of wild type PAO with (A) N1-acetyl-N3-pentyl-1,3-diaminopropane (●), 1,8-diaminooctane (□), and N1-acetyl-1,8-diaminooctane (▲) and (B) N1-acetyl-1,12-diaminododecane (■) and 1,12-diaminododecane (○). The lines for N1-acetyl-1,8-diaminooctane and N1-acetyl-1,12-diaminododecane are from fits to eq 2.1, for N1-acetyl-N3-pentyl-1,3-diaminopropane to eq 2.2, and for 1,8-diaminooctane and 1,12-diaminododecane to eq 2.3.

pH Dependence of Flavin Reduction. To address the effect of pH on catalysis rather than binding, stopped-flow spectroscopy was used to determine the rate constant for flavin reduction by N1-acetylspermine as a function of pH. Reactions were carried out at 20 ºC instead of 30 ºC because much of the reaction occurred in the dead time of the instrument at the higher temperature. Over the pH range 6.5-9.5, the flavin absorbance at 458 nm showed the same behavior: an initial decrease in absorbance, a slower, slight increase in absorbance, and finally a slow decrease in absorbance (Figure 2.4A). Data could not be obtained at pH 10 and above due to enzyme instability. The same kinetic behavior was seen when the reaction was monitored from 320-600 nm by photodiode array spectroscopy; this approach also allowed the spectra of the intermediates to be obtained (Figure 2.4B). The initial fast phase of the reaction accounts for the majority of the change in amplitude and has a rate constant that is dependent on substrate concentration (Figure 2.4C). This phase can be attributed to the rapid and reversible binding of N1-acetylspermine with no detectable change in the flavin spectrum, followed by flavin reduction. The slowest two rate constants are independent of substrate concentration and slower than k_{cat} (Figure 2.4C); therefore, they are not relevant to catalysis.

The effect of pH on the rate constant for reduction of PAO at saturating concentrations of N1-acetylspermine (k_{red}) is shown in Figure 2.5. The value of this kinetic parameter shows a decrease at acidic pH with a pK_a of 7.3 ± 0.1, indicating that a group in the ES complex must be unprotonated for reduction. Flavin reduction is

significantly faster than k_{cat} over the pH range investigated, so that the oxidative half reaction is rate-limiting for turnover with this substrate.

K315M PAO. Figure 2.6 shows the relative positions of the FAD and the conserved active site lysine in the structures of several members of the MAO structural family. Based on sequence alignment, PAO Lys315 corresponds to this conserved residue. The location of this lysine with respect to the flavin makes it a potential source of a pK_a in the k_{cat}/K_{amine}- and k_{red}-pH profiles. Consequently, the mutation K315M was introduced into PAO. The circular dichroism spectrum of the mutant protein did not reveal any significant changes compared to wild-type PAO, suggesting the K315M mutation does not affect the overall folding of the protein or the flavin environment (data not shown). The K_M value for N1-acetylspermine is less than 10 μM for the mutant protein (data not shown), so the k_{cat}/K_{amine}-pH profile for this mutant was only determined using the substrate spermine. The $k_{cat}/K_{spermine}$ value for K315M PAO is identical to that for wild-type PAO over the entire pH range (Figure 2.1A, Table 2.1), resulting in an identical pK_a of 10.3. Thus, Lys315 is not critical for polyamine oxidation, and ionization of Lys315 does not contribute to the k_{cat}/K_{amine}-pH profile.

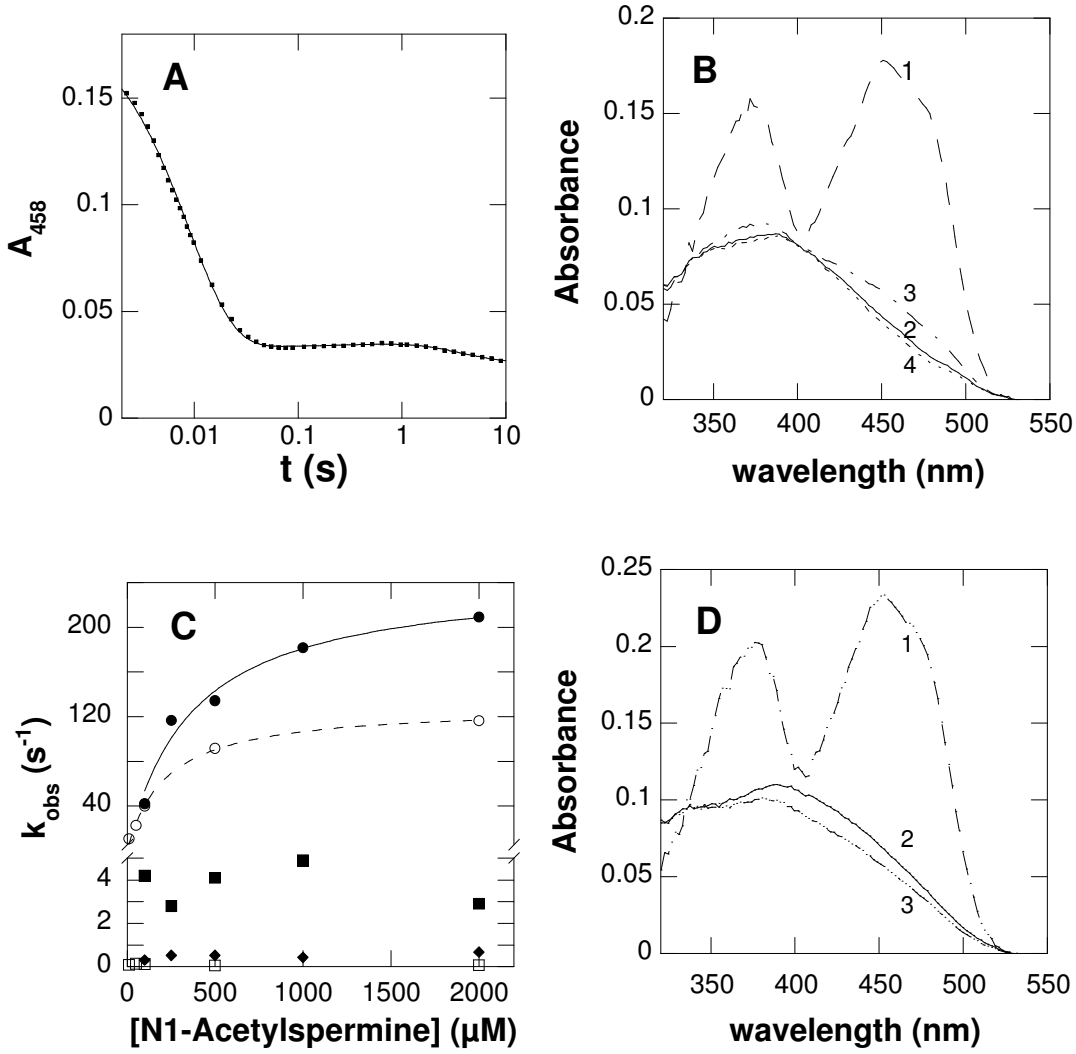

Figure 2.4: The reduction of PAO by 1 mM N1-acetylspermine at pH 7.5, 20 ºC. (A) Absorbance changes at 458 nm upon reduction of 20 μM wild-type PAO by 1 mM N1-acetylspermine. The line is from a fit to eq 2.4. (B) Absorbance spectra of flavin intermediates observed in the reductive half reaction of wild-type PAO. (C) The dependence of the individual rate constants on the N1-acetylspermine concentration for wild-type (first phase(●), second phase (■) and third phase (♦)) and K315M (first phase (○) and second phase (□)) PAO. The lines are from fits of the concentration dependence on the rate constant for the first phase to the Michaelis-Menten equation. (D) Absorbance spectra of the flavin intermediates observed in the reductive half reaction of K315M PAO.

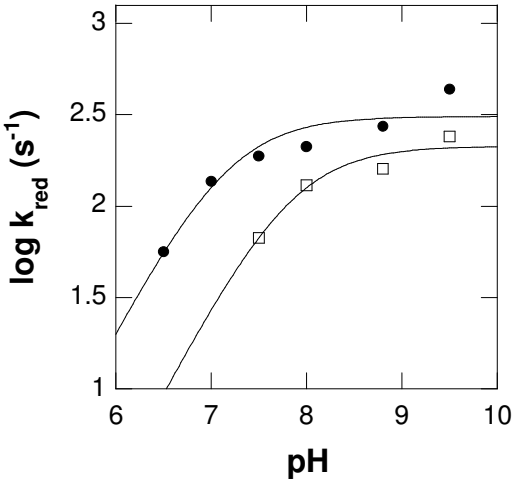

Figure 2.5: pH dependence of k_{red} for wild type (●) and K315M (□) PAO with N1-acetylspermine at 20 ºC. The lines are from fits of the data to eq 2.2.

To further investigate the role of Lys315 in catalysis, the effect of pH on the value of k_{red} with N1-acetylspermine was determined for the mutant protein. The changes in the flavin spectrum upon reduction of K315M PAO are biphasic, with a fast phase exhibiting a large change in absorbance and a slower phase exhibiting a smaller amplitude (Figure 2.4C). As with the wild-type enzyme, the rate constant for the fast phase shows a dependence on substrate concentration, while the rate constant for the slow phase is independent of substrate concentration and is slower than the k_{cat} value for the mutant protein (Figure 2.4C). At pH 9.5, the value of k_{red} is not decreased substantially from the value for the wild-type enzyme (240 s^{-1} versus 440 s^{-1}), indicating that this mutation does not have a significant effect on the reductive half reaction. The k_{red}-pH profile for K315M PAO is similar to that observed for the wild-type enzyme, with a basic shift in the pK_a to 7.8 ± 0.1 (Figure 2.5).

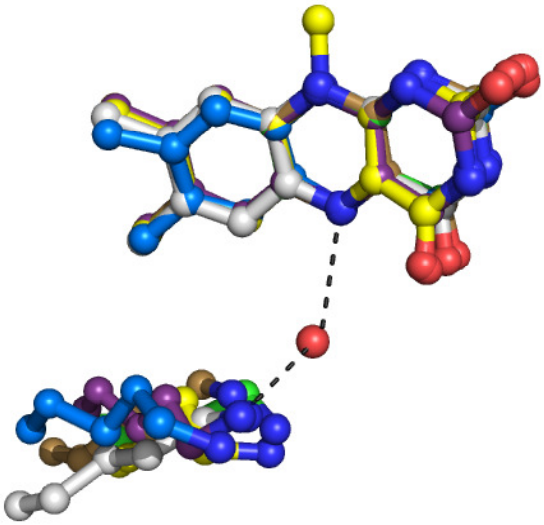

Figure 2.6: Relative positions of the conserved active site lysine and the FAD in human MAO A (blue carbons), human MAO B (purple carbons), maize PAO (yellow carbons), *S. cerevisiae* spermine oxidase Fms1 (green carbons), *Calloselasma rhodostoma* L-amino acid oxidase (gray carbons), and human LSD1 (light brown carbons). This figure was composed from PDB files 2BXS (MAO A), 1OJ9 (MAO B), 1H83 (maize PAO), 1RSG (Fms1), 1F8S (L-amino acid oxidase), and 2HKO (LSD1). To generate the figure, the atoms of the central pyrazine rings of the FAD cofactors were overlaid. The water molecule shown is from maize PAO.

DISCUSSION

The protonation state of the amine substrate required for productive binding has been a subject of controversy among those studying flavin amine oxidases. For example, Harris et al. (*69*) proposed for DAAO that a coupled deprotonation/dehydrogenation of the protonated substrate occurs in which a proton is transferred to the solvent. However, Denu and Fitzpatrick (*47*) reported that DAAO does not show a solvent isotope effect, leading to the conclusion that the amino group of the substrate must be uncharged. Further evidence for the amine being in the neutral form was provided by measurement of ^{15}N isotope effects for DAAO, which indicated that the amino group must be unprotonated for catalysis (*48*). Zhao and Jorns (*82*) subsequently concluded from studies of monomeric sarcosine oxidase that the amine substrate within the enzyme-substrate complex must be unprotonated for flavin reduction. The situation with the MAO/PAO family has been less clear. Jones et al. (*71*) concluded that uncharged inhibitors bind MAO A better, but the predominant species of the amine in the pH range of 7-9 is protonated and therefore must be the substrate. In contrast, Dunn et al. (*83*) concluded from kinetic isotope and pH studies with MAO A that deprotonation of the amine is required for catalysis. The studies reported here clearly show that mammalian PAO requires that the N4 nitrogen next to the site of CH bond cleavage be unprotonated for CH bond cleavage to occur. This is consistent with the results of Dunn et al. (*83*) with MAO, establishing that the enzymes of the MAO/PAO family all require an unprotonated nitrogen for amine oxidation, as do the members of the DAAO/sarcosine oxidase family. This requirement for a substrate with a neutral nitrogen extends the

mechanistic similarities of these two structural classes of flavin amine oxidases, a clear example of convergent evolution of enzyme mechanisms.

Comparison of the effect of pH on the protonation state of each substrate with its k_{cat}/K_{amine}-pH profiles establishes that the monoprotonated forms are required for catalysis. More specifically, the pK_i-pH profiles for the inhibitors establish that these pK_as can be attributed to specific nitrogens in the substrates. In N1-acetylspermidine, the nitrogen next to the carbon being oxidized must be unprotonated and the N10-nitrogen must be protonated. N1-Acetylspermine and spermine are more complicated due to the increased number of nitrogens. For N1-acetylspermine the N4-nitrogen must be unprotonated, but the data for the inhibitors do not establish whether it is the N10- or N14-nitrogen that must be protonated. However, the k_{cat}/K_{amine} values for N1-acetylspermine and N1-acetylspermidine are identical at the pH optimum, suggesting that it is the N10-nitrogen that is protonated, as is the case for N1-acetylspermidine. A similar case can be made for spermine. These results suggest that both protonated and unprotonated forms of the substrate can bind, but only the protonated form can react. Thus, the pK_as in the k_{cat}/K_{amine}-pH profiles are due to the substrate and not an ionizable residue within the active site of the enzyme.

The requirement for the monoprotonated substrate provides a potential mechanism of discrimination against spermine by PAO, since an acetyl moiety would prevent the terminal nitrogen from ionizing and thereby result in a very large increase in the fraction of substrate in the correctly protonated form. Although the k_{cat}/K_{amine} values are essentially identical at pH 10 for the two natural substrates N1-acetylspermine and

N1-acetylspermidine, at the physiological pH of approximately 8.2 (*84*), N1-acetylspermine is the far better substrate at physiological pH. Compared with N1-acetylspermidine, N1-acetylspermine has a broader pH profile (Figure 2.1A). This is most readily explained by a difference in the forward commitments of the two substrates, with N1-acetylspermine being a more sticky substrate.

The k_{red}-pH profile for wild type PAO shows a pK_a of 7.3 with N1-acetylspermine as substrate. The pH profile for k_{red} reports on the protonation states of ionizable groups in the enzyme-substrate complex required for reduction. The decrease in activity at acidic pH can be attributed to the substrate bound to the enzyme. The incorrectly protonated form of the substrate must be able to bind but not to react. If one assumes that substrate binding is at equilibrium, a likely oversimplification, the difference between the pK_a of the reactive nitrogen when bound to the enzyme and free in solution of 2.1 establishes that the correctly protonated form binds about 100-fold more tightly than the form with N4 protonated. Monomeric sarcosine oxidase and MAO A show similar perturbations of the amine pK_a upon binding (*82, 83*), suggesting that the active sites of these enzymes also preferentially bind the form of the substrate with the critical nitrogen in its neutral form.

Although numerous mechanisms have been put forth for flavin amine oxidases, most recent data support the mechanism as direct hydride transfer. Kinetic studies using ^{15}N isotope effects have ruled out the possibility of a polar nucleophilic addition mechanism (*49, 51*). The ^{15}N isotope effects are consistent with a single electron transfer mechanism, but the failure to detect any intermediate with a natural substrate for any

flavin amine oxidase and the very unfavorable redox change for single electron transfer from an amine to an oxidized flavin provide arguments against such a mechanism. Reduction of wild-type PAO by N1-acetylspermine shows multiple phases, with the rate constant for the fastest phase reflecting amine oxidation, while the slower phases are likely due to product release from reduced enzyme, a step that is not significant during turnover in the presence of oxygen. More critically the flavin spectrum showed no intermediate between fully oxidized and fully reduced flavin during reduction of wild type PAO by N1-acetylspermine over the entire pH range studied, indicating that oxidation of the amine substrate to the imine occurs in a single step. This result is consistent with what has been observed with other flavin amine oxidases (*45, 69, 85, 86*).

The conserved active site lysyl residue in flavin amine oxidases provides a potential source of a pK_a in the k_{cat}/K_{amine} profile. The role of this residue has previously been examined in several members of this family. In maize PAO, when Lys300 is similarly mutated to a methionine, a 1400-fold decrease in k_{red} is observed, suggesting an important but undefined role for this residue in substrate oxidation (*59*). The corresponding K661A mutation in human LSD1 completely abolished demethylase activity (*87*). In contrast, the substitution of methionine for this lysine in PAO results in no change in the k_{cat}/K_{spm} value or the pH profile with spermine, and the rate constant for flavin reduction by N1-acetylspermine shows only a 1.8-fold decrease at pH 9.5. This rules out Lys315 acting as an active site base in mouse PAO or playing any other critical role in the reductive half-reaction. The k_{red}-pH profile for K315M PAO shows a slight

basic shift in the pK_a as compared to that for wild type PAO; this can be attributed to a change in the active site environment due to the loss of the charged lysine. The reasons for the differences in the effects of mutating this residue among the different flavin amine oxidases is not apparent. It may be that this residue plays a critical role in positioning the flavin or otherwise stabilizing the active site structure, and that different flavin amine oxidases simply tolerate the loss of this interaction more than others.

In conclusion, the present study establishes the protonation state of the amine required for productive binding to PAO, and presumably for the other members of the MAO/PAO family. The results will be of use in further studies of the mechanism of amine oxidation, for interpretation of the effects of site-directed mutagenesis, for design of inhibitors, and for understanding the different substrate specificities and reactivities of polyamine and spermine oxidases. The results rule out a critical role for Lys315 in polyamine oxidation and further support hydride transfer from the neutral amine as the mechanism of flavin amine oxidases.

CHAPTER III

LYS315 PLAYS A ROLE IN THE OXIDATIVE-HALF REACTION IN MAMMALIAN POLYAMINE OXIDASE

Polyamine levels have been correlated to cell growth and differentiation and tumor growth (*8, 15, 54*) necessitating a better understanding of polyamine levels and the enzymes that regulate their corresponding levels. Polyamine oxidase (PAO) plays an important role in polyamine homeostasis, specifically by catalyzing the oxidation of N1-acetylspermine (Figure 1.3) and N1-acetylspermine to produce spermine and putrescine, respectively. PAO is of particular interest because its N1-acetylated polyamine substrates are not found in normal cells because they are the main polyamines exported from the cell (*13*). However, cancer cells display higher concentrations of N1-acetylated polyamines indicating a direct link between changes in polyamine metabolism and carcinogenesis (*14, 15*), and leading to interest in exploring the role of PAO as an anti-cancer drug target.

PAO is a flavoprotein amine oxidase that contains a non-covalently bound FAD. The general mechanism for flavoprotein amine oxidases including PAO, can be divided into two half-reactions (Figure 1.4). The reductive half-reaction consists of the transfer of a hydride equivalent from the substrate to the flavin, producing reduced flavin and oxidized amine. This step is essentially irreversible; therefore, steady-state kinetic analysis is simplified since the k_{cat}/K_m value for the amine substrate is independent of the oxygen concentration. The oxidative half-reaction involves the oxidation of reduced

flavin by molecular oxygen forming H_2O_2; thus the k_{cat}/K_{O2} value is the second order rate constant for the bimolecular reaction with reduced enzyme and oxygen.

To date, no structures for mammalian PAOs have been described. As a result, site-directed mutagenesis provides the only approach to identify residues important for catalysis. Structures of other members of the MAO flavoprotein amine oxidase structural family, including MAO-A (*76*), MAO-B (*75*), maize PAO (*73*), lysine-specific demethylase 1 (LSD1) (*32*), and Fms1, a yeast spermine oxidase (*74*), serve as a basis to design PAO mutants. Alignment of sequences of members of the MAO structural family reveal a conserved lysine in the substrate binding domain of PAO that is highly conserved throughout this family (Figure 3.1), and structural alignments show that this residue is spatially conserved as part of a "Lys-H_2O-N5" structural motif (Figure 2.6). Earlier studies of the role of Lys315 in mouse PAO indicated that the residue does not play a critical role in the reductive half-reaction (Chapter II), contrary to observations with maize PAO (*59*) and LSD1 (*87*).

Though the members of the MAO structural family contain the conserved active site lysyl residue, flavoprotein amine oxidases that belong to the D-amino acid oxidase structural family do not. Though it is unclear why the loss of this lysyl residue is better tolerated in PAO (Chapter II) than maize PAO (*59*) or LSD1 (*87*), it could be postulated that residue plays a structural role rather than a catalytic one. The studies presented here are aimed at establishing the role of Lys315 in the mechanism of PAO.

```
Mouse PAO       FEPPLPAKKAEAIKKLGFGTNNKIFLEFEEPFW
Human SMO       FRPGLPTEKVAAIHRLGIGTTDKIFLEFEEPFW
MAO-B           FNPPLPMMRNQMITRVPLGSVIKCIVYYKEPFW
MAO-A           FRPELPAERNQLIQRLPMGAVIKCMMYYKEAFW
Maize PAO       FKPKLPTWKVRAIYQFDMAVYTKIFLKFPRKFW
Fms1            FQPPLKPVIQDAFDKIHFGALGKVIFEFEECCW
                * * *                 *         *
```

Figure 3.1: ClustalW multiple sequence alignments of the substrate binding domain for mouse PAO, human spermine oxidase, human MAO-B, human MAO-A, maize PAO, and Fms1. Conserved residues are in bold.

EXPERIMENTAL PROCEDURES

Materials. Spermine was purchased from Acros Organics (Geel, Belgium) and N1-acetylspermine was purchased from Fluka (Switzerland). Deuterium oxide was purchased from Cambridge Isotope Laboratories, Inc (Andover, MA).

Expression and Purification of K315M. Wild type and K315M PAO were expressed and purified as previously described (Chapter II).

Assays. Steady-state kinetic assays were performed in air-saturated buffers conducted on a computer-interfaced Hansatech (Hansatech Instruments) electrode. Assays that required varying the concentration of oxygen was done by bubbling nitrogen in the Hansatech electrode chamber containing buffer and polyamine substrate. All assays were initiated by the addition of enzyme. All buffers contained 10% glycerol; 50 mM PIPES, 50 mM Tris-HCl, 50 mM CHES and 50 mM CAPS were used for the pH ranges of 6.6, 7.1-8.6, 9.1-9.6, and 10, respectively. Solvent isotope effects were performed in buffers containing 50 mM CHES (pH 9 or pD 9.4) or 50 mM CAPS (pH 10, or pD 10.4) with a viscosity of 1.3 prepared in either H_2O or D_2O. Glycerol buffer with a viscosity of 1.3 was prepared as established by Segur and Oberstar (*88*). A concentration of 1 mM N1-acetylspermine was used in all assays. Due to the hygroscopic nature of N1-acetylspermine, the concentration of substrate was determined enzymatically.

Data Analysis. Steady-state kinetic parameters were determined based on fits to the Michaelis-Menten equation using the program KaleidaGraph (Adelbeck Software, Reading, PA). Data for the k_{cat}/K_{O2}-pH profile of wild type PAO was fit to equation 3.1,

which applies for a kinetic parameter that decreases below pK_1 due to the protonation of a single moiety, y is the kinetic parameter being measured, c is the pH-independent value, and K_1 is the ionization constant for a residue which must be unprotonated. Eqs 3.2 and 3.3 were used to fit the proton inventories for wild type and K315M PAO, respectively. Eq 3.2 describes a linear proton inventory arising from a single proton, in which $(v/e)_n$ is the rate in air saturated buffer with a mole fraction of D_2O *n*, $(v/e)_0$ is the rate in H_2O, and KIE denotes the calculated isotope effect. Eq 3.3 describes a proton inventory of a solvent isotope effect that is due to the reactant.

$$\log y = \log (c/(1 + H/K_1)) \quad (3.1)$$

$$(v/e)_n = (v/e)_0*(1-n+(n/KIE)) \quad (3.2)$$

$$(v/e)_n = (v/e)_0/(1-n+(n/KIE)) \quad (3.3)$$

RESULTS

k_{cat}/K_{O2}-pH profile. Table 1 shows the kinetic parameters for wild type PAO at pH 8 and 10. Steady-state kinetic assays were performed using 1 mM of N1-acetylspermine while varying the concentration of oxygen over the pH range of 6.6-10. The resulting k_{cat}/K_{O2}-pH profile for wild type PAO is shown in Figure 3.2 and shows a pK_a of 7.0 ± 0.1 with a decrease in activity at acidic pH.

Solvent Isotope Effects and Proton Inventory. Experiments to determine the solvent isotope effect on the kinetic parameter k_{cat}/K_{O2} for wild type PAO were performed at pH 10 (Figure 3.3A) and result in a value of 1.43 ± 0.05. To test whether this is a true solvent isotope effect and not due to the viscosity of the D_2O buffer, the effect of 10% (w/w) glycerol on the k_{cat}/K_{O2} value was determined. This concentration of glycerol results in η equal to 1.3, the viscosity of D_2O. The activity increased in the presence of glycerol, for an inverse viscosity effect of 0.85 ± 0.03. This establishes that the decrease in k_{cat}/K_{O2} in D_2O is not due to the viscosity of the D_2O solution. Next, a proton inventory was conducted at pH 10 and pD 10.4 (Figure 3.4A) in an effort to determine the number of protons responsible for the observed isotope effect. Data from this experiment was best fit to a linear dependence of the rate on the mole fraction of D_2O, indicating this solvent isotope arises from a single exchangeable proton.

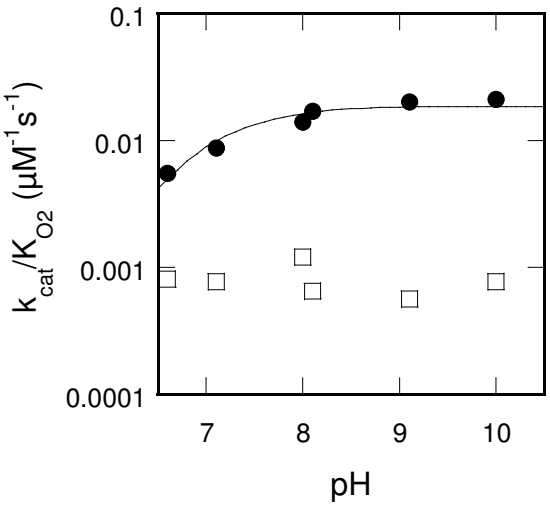

Figure 3.2: The k_{cat}/K_{O2}-pH profile for wt (●) and K315M (□) PAO with N1-acetylspermine. The line is from the fit of data to eq 3.1.

Table 3.1: Steady-state kinetic parameters for wild type and K315M PAO with 1 mM N1-acetylspermine and varied concentrations of oxygen.

	pH 8			**pH 10**		
PAO	**k_{cat}/K_{O2} ($\mu M^{-1} s^{-1}$)**	**K_{O2} (μM)**	**k_{cat} (s^{-1})**	**k_{cat}/K_{O2} ($\mu M^{-1} s^{-1}$)**	**K_{O2} (μM)**	**k_{cat} (s^{-1})**
Wild type	0.014 ± 0.001	318 ± 47	4.3 ± 0.2	0.021 ± 0.003	990 ± 250	20.5 ± 2.6
K315M	0.0012 ± 0.0001	1000 ± 120	1.2 ± 0.1	0.00077 ± 0.00012	5960 ± 5950	4.5 ± 3.8

*Conditions: 0.05 mM TRIS (pH 8) or CAPS (pH 10), 10% glycerol, 20º C

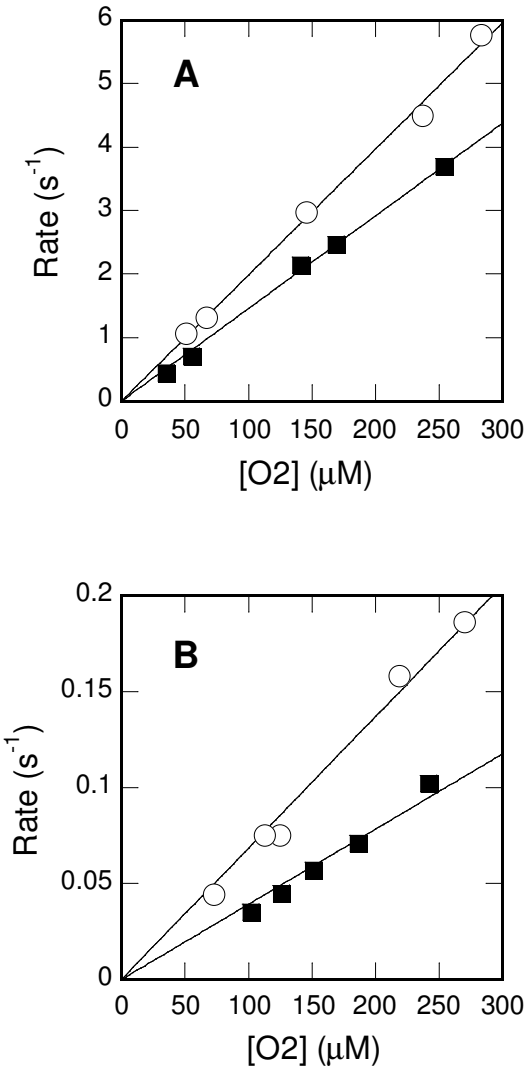

Figure 3.3: Solvent isotope effects on k_{cat}/KO_2: (A) wild type and (B) K315M PAO in H_2O (○) and D_2O (■) at pH 10 or pD 10.4, 20ºC with 1 mM N1-acetylspermine.

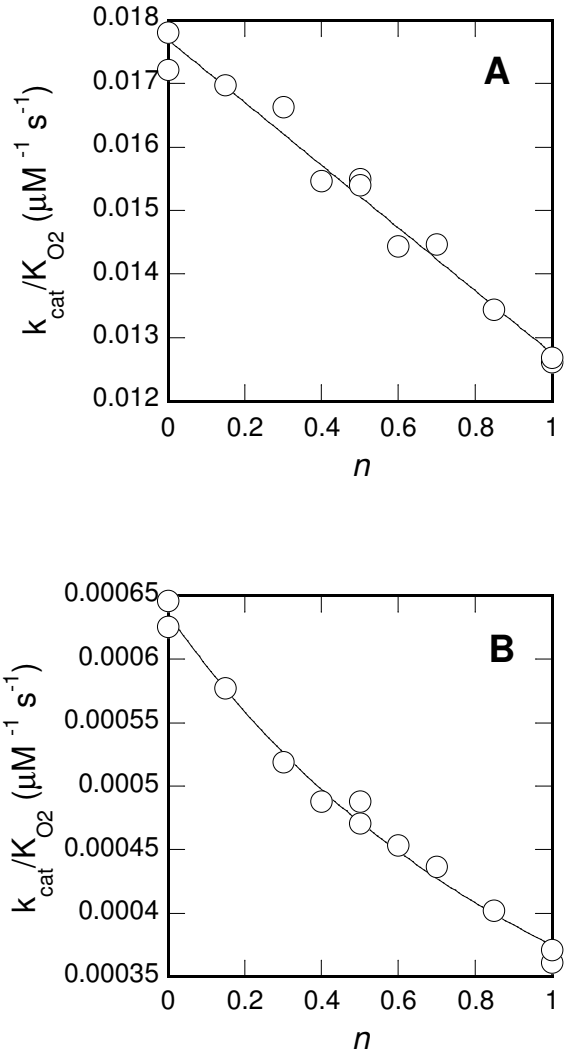

Figure 3.4: Proton inventories of wild type and K315M PAO. The effect of the mole fraction of D_2O, *n*, on the rate of N1-acetylspermine oxidation in air-saturated buffer at pH 10, pD 10.4 for (A) wild type and (B) K315M PAO. Lines are from fits to eq 3.2 for wild type and to eq 3.3 for K315M PAO.

K315M Mouse PAO. To determine the effect the K315M mutation has on the oxidative half-reaction, steady-state kinetic assays were performed using 1 mM of N1-acetylspermine while varying the concentration of oxygen over the pH range of 6.6-10. The resulting k_{cat}/K_{O2}-pH profile for K315M PAO is shown in Figure 3.2. These results show that with K315M PAO, k_{cat}/K_{O2} is pH –independent and reduced about 30-fold in value with respect to the wild-type enzyme. In assessing steady-state parameters shown in Table 3.1, the effect the K315M mutation has on k_{cat}/K_{O2} is more significant and pH-dependent, whereas on k_{cat} the effect is only 4-to-5-fold and pH-independent. However, the k_{cat} value cannot be measured accurately due to the inability to saturate the enzyme with oxygen at pH 10.

The solvent isotope effect at pH 10 has a value of 1.84 ± 0.08. To ensure that data was collected in a pH-insensitive region, the solvent isotope effect was also determined at pH 9 giving a value of 1.98 ± 0.05. These values are within error of each other and give an average solvent isotope effect of 1.91 ± 0.06. The proton inventory for the rate of oxidation of N1-acetylspermine at pH 10 for K315M, in contrast to wild type enzyme, shows a bowl-shaped curve that is concave up and is best fit to eq 3.3 giving an R^2 value of 0.99. Eq 3.3, which attributes the solvent isotope effect as being due to a reactant, gives a better fit than other equations which indicate a solvent isotope effect arising from a single proton, two protons with equal isotope effects, or a large number of protons, each of which give fits with an R^2 of 0.98 or less.

DISCUSSION

Structural information compiled from crystal structures of various flavin amine oxidases presents the opportunity to investigate the functional importance of structural motifs in PAO. One such motif is the hydrogen bond network that exists between a conserved lysyl residue in the active site to the N5 atom of the FAD cofactor via a water molecule. When the lysine of this "Lys-H_2O-N5" structural motif was mutated to a methionine in maize PAO, the rate constant for flavin reduction was reduced 1400-fold (*59*). Similarly, the Lys661Ala mutation in LSD1 abolished demethylase activity (*32*). The effect of the K315M mutation in PAO on the reductive half-reaction has been the source of earlier study, showing modest effects in the rate of flavin reduction (Chapter II).

In an effort to better understand the oxidative half reaction, results of wild type PAO studies show that k_{cat}/K_{O2} is pH-dependent with an increase in activity observed at higher pH. This result indicates that deprotonation of a moiety within the enzyme enhances oxidation. To better understand the role of the conserved Lysine residue found in the active site of members of the MAO structural family, the mutant K315M was characterized. K315M PAO shows k_{cat}/K_{O2} values that are depressed in comparison to wild type and are pH-independent (Figure 3.2, Table 3.1). From these results, two conclusions can be drawn. First, Lys315 plays a role in the oxidative half-reaction, though not a critical one. Second, the deprotonation in wild type PAO with a pK_a of 7.0 ± 0.1 is due to the protonation of Lys315. The mutant still maintains the ability to oxidize substrate, a decrease that is greater than an order of magnitude is observed in the

k_{cat}/K_{O2} rate constant, with a smaller 4-to-5-fold effect observed for k_{cat} (Table 3.1). The results seen in the oxidative half-reaction are in contrast to the modest 1.5-fold decrease observed for the rate of flavin reduction with N1-acetylspermine (Chapter II). The importance positively charged residues have in establishing electrophilicity and polarity of the active site of flavoproteins is documented in the literature. In addition to the aforementioned conserved lysyl residue in members of the MAO structural family, glucose oxidase possesses His516 which plays an important role in the oxidation of reduced flavin by contributing a positive charge that facilitates the formation of O_2^- (*89*). Results with the flavoprotein choline oxidase, which catalyzes the oxidation of choline to glycine betaine, indicates involvement of two histidines, His351 and His466, both of which must be protonated for optimal catalysis and aid in transition state stabilization of the alkoxide species (*90, 91*). What is different with PAO is that it is the loss of that positive charge that enhances activity. It appears that this lysyl residue in PAO must be uncharged to hydrogen bond to water as depicted in Figure 3.5. Thus, it is postulated that the role of the hydrogen bond network between the uncharged Lys315, a water molecule, and the N5 of the flavin within PAO is to enhance the rate of oxidation of the reduced flavin. The proton bonded to the N5 atom of the flavin must be removed during oxidation of reduced flavin. It could therefore be postulated that Lys315 in PAO removes a proton from the water molecule, activating it to remove the proton bound at the N5 position, thus facilitating reformation of oxidized flavin for the next round of catalysis.

Solvent isotope effects with wild type and K315M PAO reflect a significant change occurring within the active site by removal of this lysyl residue. The increase in the solvent isotope effect seen with K315M PAO suggests that the lysyl residue is replaced with water molecules. Further evidence of this comes from the change in proton inventory of wild type PAO, which shows that a single proton is exchangeable to solvent, compared to that of K315M PAO where a significant change is observed with the simplest explanation being the presence of an additional water molecule in the active site. Though another water molecule can bind within the active site in the absence of Lys315, the inefficiency of such a replacement is reflected in a decrease by an order of magnitude in k_{cat}/K_{O2}. With PAO, previous studies indicated that under single turnover conditions a slow step is observed that is slower than turnover (Chapter II). It is probable that this is product release in the absence of oxygen; thus reduced enzyme reacts with molecular oxygen before product is released, and product release is rate-limiting. The lesser effect of 4-5 fold observed for k_{cat} with mutant enzyme reflects that the full effect of the mutation is partially masked due to another partially-rate limiting step such as product release.

The results of this study with mammalian PAO establish the role of Lys315 as being involved in a hydrogen bond network (Figure 3.5), in which the deprotonated form of Lys315 serves to enhance the rate of oxidation of reduced flavin via a water molecule. The removal of this lysyl residue results in the presence of an additional water molecule in the active site as reflected in solvent isotope effects and proton inventory. It remains unclear as to why differences exist with K300M maize PAO (*59*) as compared to

K315M mouse PAO (Chapter II) with respect to the rate of flavin reduction. Perhaps, the simplest explanation is that in maize PAO, Lys300 does not play a direct role in substrate oxidation, but rather causes enzyme instability resulting from structural effects, whereas in mouse PAO, the loss of this residue is structurally less dramatic. What can be concluded is that in mammalian PAO, this conserved lysyl residue plays a direct, though not vital, role in the oxidative half-reaction.

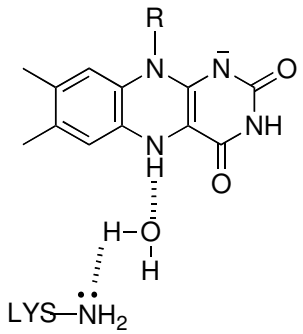

Figure 3.5: Hydrogen bond network of "Lys-H_2O-N5" motif in mammalian PAO.

CHAPTER IV

MECHANISTIC STUDIES OF PARA-SUBSTITUTED N,N'-DIBENZYL-1,4-DIAMINOBUTANES AS SUBSTRATES FOR A MAMMALIAN POLYAMINE OXIDASE

Polyamine oxidase (PAO) is a flavoprotein that plays a pivotal role in polyamine metabolism by combining biosynthesis and degradation pathways with the regulated import and export of polyamines (*92*). The activity of PAO in maintaining polyamine homeostasis indicates it has an important role in facilitating apoptosis in cancer cells (*93*). Specifically, PAO catalyzes the oxidation of N1-acetylspermine and N1-acetylspermidine to the products spermidine and putrescine, respectively, producing H_2O_2 as a by-product. Recent studies show the potential for targeting tumor cells by inducing PAO with specific polyamine analogues that leads to the cytotoxic production of H_2O_2 in a tumor specific manner, including solid tumors found in lung, breast, colon, and prostate (*94, 95*). PAO, not to be confused with a spermine oxidase, preferentially reacts with acetylated polyamines, though it can also oxidize spermine (*26*). The study presented here uses PAO from mouse, and as a distinction from plant PAOs where CH bond cleavage occurs on the *endo*-side of spermine (*63*), mammalian PAOs catalyze CH bond cleavage on the *exo*-side of the N4-nitrogen in N1-acetylspermine and N1-acetylspermidine.

PAO is a member of the flavin amine oxidase superfamily and belongs to the structural family that includes monoamine oxidase A and B (MAO-A/B) (*60*), lysine-

specific demethylase (LSD1) (*32*), L-amino acid oxidase (*34*), and tryptophan 2-monooxygenase (TMO) (*53*) amongst others. Sequence alignments reveal low sequence identity of PAO with other flavoprotein amine oxidases (*26*), though no evidence has been found to suggest that these enzymes utilize different mechanisms. The reaction of PAO, like other flavoprotein amine oxidases, can be divided into two half-reactions. The reductive half-reaction consists of substrate binding and flavin reduction upon substrate oxidation, and the oxidative-half reaction involves the oxidation of reduced flavin via molecular oxygen. The steady-state kinetic mechanism for mouse PAO displays the ping-pong kinetic pattern (*26*), as is observed with most flavoprotein oxidases (*64*). Due to the irreversibility of the reductive half-reaction, analysis of the k_{cat}/K_m parameter for the amine substrate can be conducted in air saturated buffers since its value is independent of the oxygen concentration. To determine the rate constant for flavin reduction, anaerobic rapid-reaction methods are utilized to monitor changes in the observed flavin spectrum going from oxidized to reduced.

There are multiple mechanisms that have been presented for the mode by which CH bond cleavage is achieved. Three mechanisms that have become more prominent in the discussion of flavoprotein amine oxidases include the single electron transfer mechanism (Figure 1.8) (*39*), the polar nucleophilic mechanism (Figure 1.9) (*45*), and the hydride transfer mechanism (Figure 1.10) (*49, 51, 96, 97*). In order to determine the mechanism by which PAO functions, the study described here investigates the charge

development during the transition state of oxidation by a mammalian PAO using N,N'-(4-X-benzyl)$_2$-1,4-diaminobutanes as substrates. The influence of the different substituents on the rate of oxidation of polyamine analogues varies and can be assessed in terms of steric (V_W and E_S), hydrophobic (π), and electronic properties (σ, σ^+ and σ^-). Analysis of these effects through correlations of steady-state and transient kinetic rate constants allows the opportunity to investigate the effects such groups have on the development of the charge in the chemical step during the transition state. Kinetic isotope effects as a function of pH were determined with N,N'-(4-X-benzyl)$_2$-1,4-diaminobutanes in order to gain information about the timing of CH bond cleavage during oxidation of the substrate, allowing further insight into the nature of the transition state. These results observed for PAO are compared with results of structure-activity relationships observed with MAO and are discussed in terms of the various mechanisms proposed for flavoprotein amine oxidases.

EXPERIMENTAL PROCEDURES

Syntheses. All substrates used in this study were synthesized by Dr. Vijay Gawandi of Texas A&M University.

Expression and Purification of Recombinant PAO Proteins. Cells were grown to an O.D. of 0.6 before being induced with 0.15 mM IPTG, and grown overnight at 20 °C. Cells were harvested by centrifugation at 22400 *g* for 30 min. Cell paste was resuspended in 50 mM potassium phosphate (pH 7.5), 10% glycerol, 2 μM leupeptin and pepstatin, and 100 μg/mL phenylmethanesulfonyl fluoride and lysozyme and lysed by sonication. After centrifugation at 22400 *g* for 30 min, the resulting supernatant was loaded onto a HisTrap FF precharged Ni Sepharose™ 6 Fast Flow (GE Lifesciences) column washed with ten column volumes of 50 mM potassium phosphate (pH 7.5), 10% glycerol, 0.4 M sodium chloride, 10 mM imidazole. The protein was eluted using a 20-column volume gradient of 10 mM – 200 mM imidazole. The resulting protein was pooled and concentrated by a 65% ammonium sulfate precipitation, centrifuged at 22400 *g* for 30 min, and resuspended in minimal volume of 50 mM potassium phosphate (pH 7.5), 10% glycerol, and dialyzed overnight in the same buffer. After a final centrifugation at 22400 *g* for 30 min, the purified enzyme was stored at -80 °C in 50 mM potassium phosphate (pH 7.5), 10% glycerol. The concentration of active enzyme was determined from the flavin visible absorbance spectrum using an ε_{458} value of 10,400 M^{-1} cm^{-1} (*79*).

Steady-State Assays. Steady-state kinetic parameters for PAO were determined using a computer-interfaced Hansatech Clark oxygen electrode (Hansatech Instruments).

All assays were performed at 30 ^{o}C and were initiated by addition of enzyme. The buffers used for pH range 7.1-8.6 was 50 mM Tris-HCl, 50 mM CHES at pH 9.1-9.6, and 50 mM CAPS at pH 10.1. All buffers contained 10 % glycerol. Enzyme was used to check the concentration of substrates; the concentration of substrate based on the oxygen consumption assay was twice that based on molecular weight, indicating an ability of PAO to recognize and oxidize both sides of N,N'-(4-X-benzyl)$_2$-1,4-diaminobutanes.

Rapid Reaction Kinetics. Rapid reaction kinetic measurements were performed on an Applied Photophysics SX-18MV stopped-flow spectrophotometer using both single wavelength and photodiode array detection. To establish anaerobic conditions, the instrument was loaded with anaerobic buffer containing 5 mM glucose and 36 nM of glucose oxidase and left overnight. Enzyme solutions containing 5 mM glucose were made anaerobic by applying cycles of argon and vacuum; substrate solutions containing 5 mM glucose were made anaerobic by bubbling with argon. Glucose oxidase was added to all anaerobic solutions at a final concentration of 36 nM.

Data Analysis. Data were analyzed using the programs Kaleidagraph (Adelbeck Software, Reading, PA) and Igor (WaveMetrics, Lake Oswego, OR). Initial rate data were fit to the Michaelis-Menten equation to determine steady-state kinetic parameters. The k_{cat}/K_{DBDB}-pH profile was fit to eq 4.1, where y is the value of the kinetic parameter, c is its pH-independent value, K_1 is the ionization constant for a moiety that must be unprotonated for maximum activity and K_2 is the ionization constant for a moiety that must be protonated for maximum activity.

$$\log y = \log[c/(1+H/K_1 + K_2/H)] \quad (4.1)$$

Kinetic isotope effects on steady-state parameters were determined from fits to eq 4.2 or 4.3, where E is the isotope effect on the parameters k_{cat}/K_{DBDB} and k_{cat}, s is the concentration of substrate, F_i is the fraction of heavy isotope in the substrate, and, in eq 4.3, K_{ai} is the substrate inhibition constant. Some of the substrates exhibited substrate inhibition and were consequently fit with eq 4.3.

$$v = (V*s)/((K_M+s)*(1+(E-1)*F_i) \quad (4.2)$$

$$v = (V*s)/((K_M *(1+F_i*(E-1))+s*(1+F_i*(E-1))+s^2/K_{ai}) \quad (4.3)$$

Rapid reaction kinetic traces were fit to single and double exponential decays (eqs 4.4 and 4.5); here, k_1 and k_2 are the first order rate constants, A_1 and A_2 are the

absorbance changes associated with the two phases, A_t is the total absorbance change, and A_∞ is the final absorbance.

$$A_t = A_1 e^{-k_1 t} + A_\infty \quad (4.4)$$

$$A_t = A_1 e^{-k_1 t} + A_2 e^{-k_2 t} + A_\infty \quad (4.5)$$

The k_{red}-pH profile for PAO oxidation of N,N'-(4-H-benzyl)$_2$-1,4-diaminobutanes was fit to eq 4.6, where y is the value of the kinetic parameter, y_L is the value of the low plateau in the sigmoidal curve, Δy_L is the change in rate between the high and low plateaus, and K_1 is the ionization constant.

$$\log y = \log (y_L + (\Delta y_L / (1 + H/K_1)) \quad (4.6)$$

RESULTS

N, N'-dibenzyl-diamines As Substrates. Several N, N'-dibenzyl-diamines were previously shown to be substrates for partially purified polyamine oxidase from pig liver, producing benzaldehyde as product; the highest activity was seen with the 1,3-diaminopropane and 1,4-diaminobutane derivatives (*13*). With purified recombinant mouse enzyme in hand, we determined the kinetics of oxidation of N, N'-dibenzyl-1,2-diaminoethane, N,N'-dibenzyl-1,3- diaminopropane, and N, N'-1,4-dibenzyl-diaminobutane in air-saturated buffer at pH 8.6. No activity was detected with the diaminoethane derivative. The apparent k_{cat}, K_m, and k_{cat}/K_m values for N, N'-dibenzyl-1,3- diaminopropane were 6.1 ± 0.2 s^{-1}, 40 ± 6 μM, and 0.15 ± 0.02 $\mu M^{-1}s^{-1}$, respectively. For N, N'-dibenzyl-1,4-diaminobutane, the values of these kinetic parameters were 0.80 ± 0.02 s^{-1}, 15 ± 2 μM, and 0.06 ± 0.01 $\mu M^{-1}s^{-1}$. The latter K_m value is within a factor of two of the value reported for the pig enzyme at 37 ^{o}C; the kinetic parameters for N, N'-dibenzyl-1,3-diaminopropane were not reported previously. The lower activity of N, N'-dibenzyl-1,4-diaminobutane suggested that chemistry is more likely to be rate-limiting with this compound. Consequently, analogs of this compound were selected for further study.

Steady-State Kinetics. The steady-state kinetic parameters apparent k_{cat}, k_{cat}/K_M, and K_M were determined for PAO at pH 8.6 and 30 °C for seven N,N'-(4-X-benzyl)$_2$-1,4-diaminobutanes as substrates (Table 4.1). The enzyme displays ping pong kinetics so assays were conducted in air-saturated buffers; therefore, the k_{cat} parameter calculated is

an apparent k_{cat}. All the N,N'-(4-X-benzyl)$_2$-1,4-diaminobutanes used in this study are slow substrates.

k_{cat}/K_{DBDB}-pH Profile. The steady-state kinetic parameter k_{cat}/K_{DBDB} was determined over the pH range 7.1-10.1 at 30 °C for protiated and deuterated N, N'-(benzyl)$_2$-1,4-diaminobutane, N,N'-(4-CH_3O-benzyl)$_2$-1,4-diaminobutane, and N,N'-(4-CF_3-benzyl)$_2$-1,4-diaminobutane as substrates for PAO. The resulting k_{cat}/K_M-pH profiles for all three substrates are bell-shaped curves (Figure 4.1A), decreasing below pK_1 and above pK_2. Fits to eq 1 indicate that the pK_a values for all three substrates (Table 4.2) are within error of each other, with an average value of 8.0 for pK_1 and of 10.0 for pK_2.

Table 4.1: Kinetic parameters of PAO with N,N'-(4-X-benzyl)$_2$-1,4-diaminobutanes as substrates at pH 8.6, 30 °C.

4,4'-X-DBDB	Kinetic Parameter			
para-Substituent	k_{cat} (s^{-1})	k_{cat}/K_M (μM^{-1} s^{-1})	K_M (μM)	k_{red} (s^{-1})
-OCH_3	4.5 ± 0.1	0.24 ± 0.01	19 ± 1	4.1 ± 0.6
-H	0.80 ± 0.02	0.054 ± 0.004	15 ± 2	0.76 ± 0.04
-CF_3	2.3 ± 0.1	0.53 ± 0.10	4 ± 2	1.6 ± 0.1
-$N(CH_3)_2$	10.1 ± 0.5	0.12 ± 0.02	87 ± 15	23.9 ± 0.3
-CH_3	3.8 ± 0.3	0.35 ± 0.06	11 ± 3	1.8 ± 0.1
-Cl	1.4 ± 0.1	0.97 ± 0.30	1.4 ± 0.5	0.80 ± 0.01
-Br	1.8 ± 0.1	1.0 ± 0.2	1.8 ± 0.4	1.1 ± 0.1

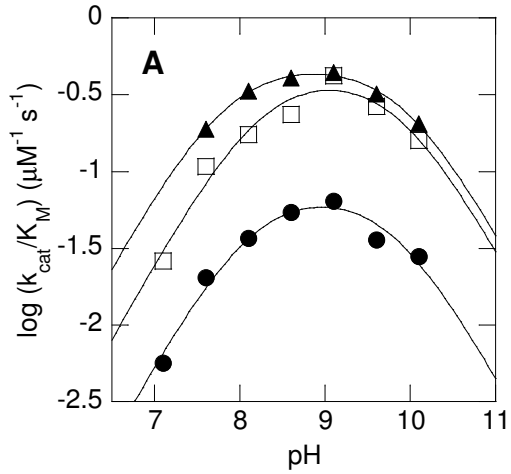

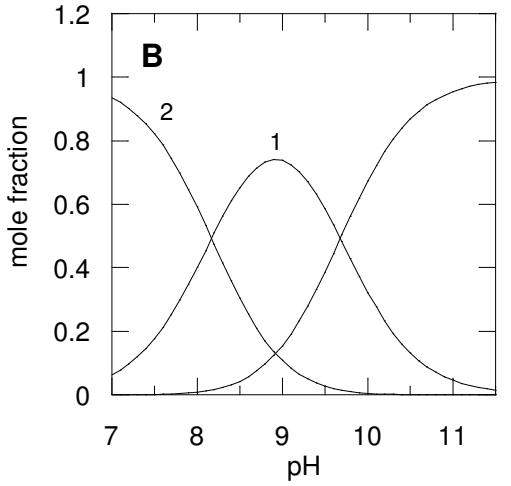

Figure 4.1: (A) k_{cat}/K_m-pH profiles of PAO with N,N'-(benzyl)$_2$-1,4-diaminobutane (●), N,N'-(4-CH_3O-benzyl)$_2$-1,4-diaminobutane (□), and N,N'-(4-CF_3-benzyl)$_2$-1,4-diaminobutane (▲) as substrates. The lines are from fits of the data to eq 4.1. (B) pH distribution of N,N'-(-benzyl)$_2$-1,4-diaminobutane with zero, one, and two protons.

Table 4.2: pK_a values for k_{cat}/K_{DBDB}-pH profiles for N,N'-(4-X-benzyl)$_2$-1,4-diaminobutanes as substrates for PAO

Substrate	**pK_{a1}**	**pK_{a2}**
4,4'-H-DBDB (protiated)	8.1 ± 0.1	9.8 ± 0.2
4,4'-H-DBDB (deuterated)	8.1 ± 0.1	10.0 ± 0.2
4,4'-CH_3O-DBDB (protiated)	8.2 ± 0.2	9.9 ± 0.2
4,4'-CH_3O-DBDB (deuterated)	8.2 ± 0.2	10.0 ± 0.3
4,4'-CF_3-DBDB (protiated)	7.8 ± 0.1	9.9 ± 0.1
4,4'-CF_3-DBDB (deuterated)	7.8 ± 0.1	10.1 ± 0.1

conditions: experiments were performed in air saturated buffers at 30 °C

Steady-State Kinetic Isotope Effects. Deuterium kinetic isotope effects were determined using di-deuterated N,N'-(4-X-benzyl)$_2$-1,4-diaminobutanes, which results in isotope effects that reflect both the primary and secondary effects. Data obtained from varying the concentration of N,N'-(4-X-benzyl)$_2$-1,4-diaminobutanes in air-saturated buffer were best fit using eq 4.2, which assigns equal isotope effects on $^{D}k_{cat}/K_{DBDB}$ and $^{D}k_{cat}$. In instances where substrate inhibition was observed, eq 4.3 was used instead. For each of the three substrates used, the isotope effect on k_{cat}/K_{DBDB} and k_{cat} is less than two and are pH independent (Table 4.3). These three substrates are representative of the different substituents from the series of the N,N'-(4-X-benzyl)$_2$-1,4-diaminobutanes used for study here, and lack of any notable changes observed in the kinetic isotope effect did not necessitate further studies with other analogues.

Flavin Reduction Kinetics. Stopped-flow experiments were conducted to determine directly the effects that *para*-substituents have on the rate of flavin reduction, k_{red}. To obtain rate constants as a function of substrate concentration, reactions were monitored at 458 nm (Figure 4.2A, closed symbols); with the majority of the substrates, the spectral changes upon mixing enzyme and substrate could be fit to a single exponential decay. The exception was N,N'-(4-N(CH_3)$_2$-benzyl)$_2$-1,4-diaminobutane; in this case the traces were fit better to a double exponential decay (Figure 4.2A, closed symbols), where the second rate constant is slower than turnover and therefore not catalytically relevant. These experiments were conducted at both pH 8.6, near the pH optimum, and at pH 6.6. Experiments at pH 9.6 were attempted, but enzyme instability at such a high pH prevented the acquisition of usable data. For each substrate, a

photodiode array detector was used to monitor the spectral changes during the course of the reaction (Figure 4.2B). Global analyses of the data showed that flavin reduction occurs in a single step, with no observable intermediates between fully oxidized and fully reduced flavin (Figure 4.2C). These results are summarized in Table 4. Similar analyses were carried out with the deuterated substrates; the resulting isotope effects on the k_{red} values range from 1.3 to 2.9 for N,N'-(4-X-benzyl)$_2$-1,4-diaminobutane substrates and are pH independent (Table 4.4). The isotope effects on k_{red} are comparable to those on k_{cat}/K_m and k_{cat}.

The pH-profile of the rate of flavin reduction with the substrate N'-(benzyl)$_2$-1,4-diaminobutane is a sigmoid curve with an increase in activity at higher pH (Figure 4.3). Deprotonation of a group within the ES complex having a pK_a of 8.2 ± 0.3 results in an increase in activity of approximately 4-fold. The rate constant at low pH is 0.20 ± 0.01 s^{-1} and at high pH is 0.82 ± 0.13 s^{-1}.

Table 4.3: Effect of pH on the $^{D}(k_{cat}/K_m)$ and $^{D}k_{cat}$ values for N,N'-(4-X-benzyl)$_2$-1,4-diaminobutanes as substrates for PAO

pH	**Kinetic Isotope Effects**		
	X = H	**X = CH_3O**	**X = CF_3**
7.1	1.3 ± 0.1	1.7 ± 0.1	n.d.
7.6	1.7 ± 0.1	1.8 ± 0.1	1.4 ± 0.1
8.1	1.8 ± 0.1	1.7 ± 0.1	1.5 ± 0.1
8.6	2.0 ± 0.1	1.7 ± 0.1	1.6 ± 0.1
9.1	2.1 ± 0.2	1.7 ± 0.1	1.5 ± 0.1
9.6	2.0 ± 0.2	1.6 ± 0.1	1.6 ± 0.1
10.1	1.9 ± 0.1	1.6 ± 0.1	1.6 ± 0.1
Average	**1.8 ± 0.3**	**1.7 ± 0.1**	**1.5 ± 0.1**

n.d. not determined

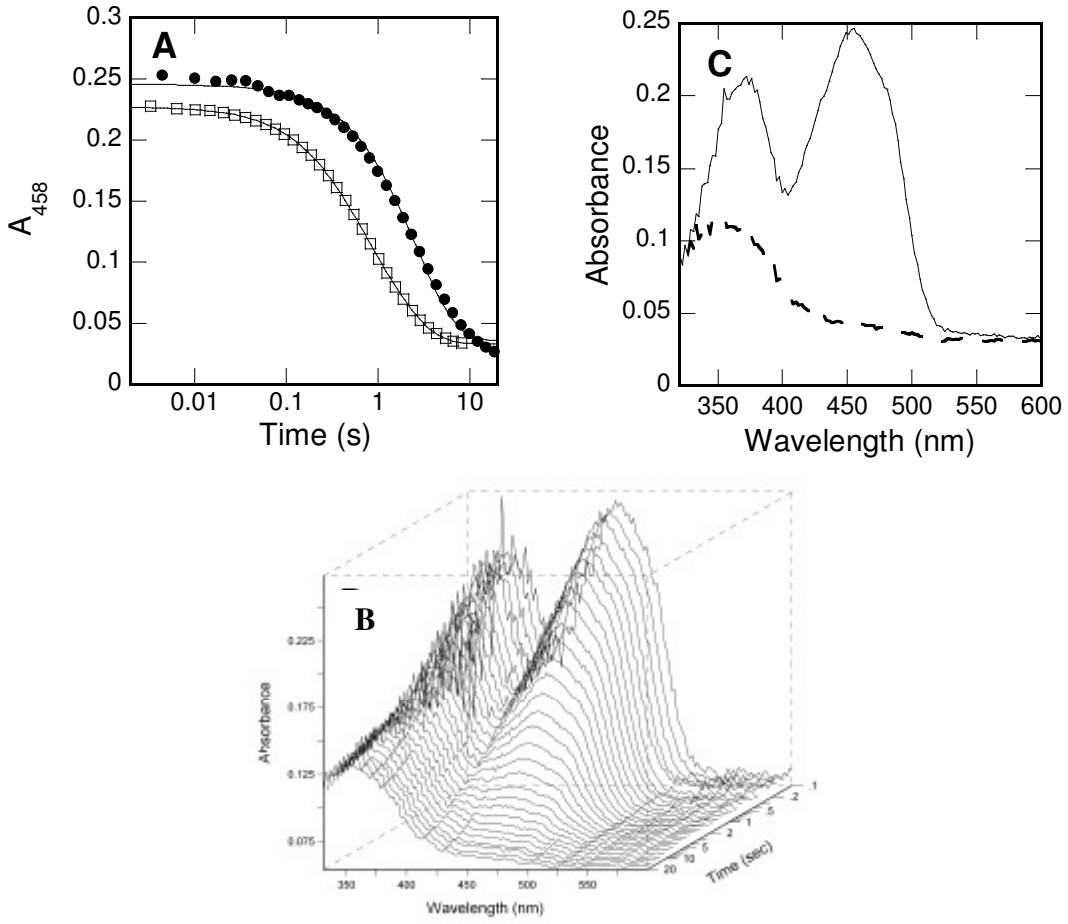

Figure 4.2: Spectral changes during reduction of PAO by N,N'-(4-X-benzyl)$_2$-1,4-diaminobutanes at pH 6.6, 30 °C. (A) time course of reduction by 2 mM N,N'-(4-CH_3-benzyl)$_2$-1,4-diaminobutane (filled symbols) and 0.1 mM N,N'-(4-N(CH_3)$_2$-benzyl)$_2$-1,4-diaminobutane (open symbols); only 1/30th of the points are shown for clarity; (B) changes in the entire visible absorbance spectrum during reduction by 2 mM N,N'-(4-CH_3-benzyl)$_2$-1,4-diaminobutane; (C) initial (—) and final (···) spectra upon flavin reduction from a global analysis of the data in B using a single-step kinetic model. The lines in A are from fits of the data to eq 4.4 for N,N'-(4-CH_3 -benzyl)$_2$-1,4-diaminobutane and eq 4.5 for N,N'-(4-N(CH_3)$_2$ -benzyl)$_2$-1,4-diaminobutane.

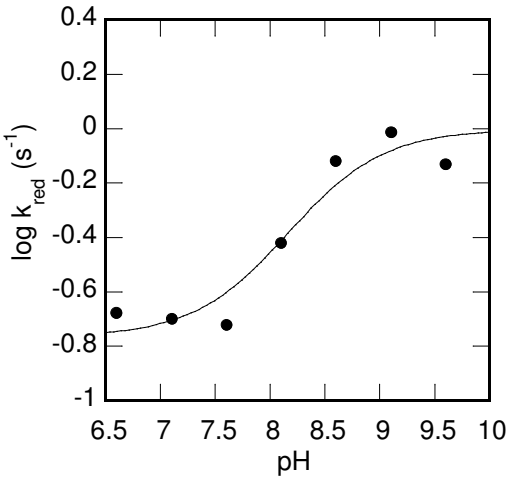

Figure 4.3: pH dependence of k_{red} for PAO oxidation of N,N'-(benzyl)$_2$-1,4-diaminobutane at 30 °C. The line is from a fit to eq 4.6.

Table 4.4: Rate constants and deuterium kinetic isotope effects for reduction of PAO by substituted N,N'-(4-X-benzyl)$_2$-1,4-diaminobutanes.

	pH 6.6		**pH 8.6**	
Substituent	**k_{red} (s^{-1})**	**$^{D}k_{red}$**	**k_{red} (s^{-1})**	**$^{D}k_{red}$**
-$N(CH_3)_2$ [a]	2.8 ± 0.3	1.4 ± 0.2	23.9 ± 0.6	1.7 ± 0.1
-OCH_3 [b]	1.19 ± 0.01	1.8 ± 0.1	4.1 ± 0.6	1.6 ± 0.2
-CH_3 [b]	0.66 ± 0.01	1.7 ± 0.1	1.84 ± 0.01	1.8 ± 0.1
-H [b]	0.21 ± 0.01	1.8 ± 0.1	0.42 ± 0.02	1.5 ± 0.1
-Cl [b]	0.48 ± 0.01	2.2 ± 0.1	0.80 ± 0.02	2.9 ± 0.1
-Br [b]	0.56 ± 0.02	1.7 ± 0.1	1.04 ± 0.06	1.5 ± 0.1
-CF_3 [b]	1.05 ± 0.02	1.8 ± 0.1	1.58 ± 0.06	1.3 ± 0.1

[a] Data fit to eq 4.5
[b] Data fit to eq 4.4

Linear Correlation Analysis. The effect of the substituent at the *para*-position of the aromatic rings on the rate constant for flavin reduction can be analyzed using single- or multiple-parameter linear correlations with electronic (σ, σ^+, σ^-), hydrophobic (π), and steric parameters (V_W and E_S, where V_W is the van der Waals volume and E_S is the Taft steric parameter). Eq 4.7 describes a single-parameter linear correlation where ρ is the parameter coefficient for the σ parameter and C is a constant. Eq 4.8 describes a two-parameter linear correlation where ρ and A are the coefficients for the two-parameters being analyzed.

$$\log k_{red} = \rho\sigma + C \qquad (4.7)$$

$$\log k_{red} = \rho\sigma + A\pi \text{ (or } V_W \text{ or } E_S) + C \qquad (4.8)$$

The results of the analyses are summarized in Table 4.5. The best single-parameter correlation is with the van der Waals volume at both pH 8.6 and 6.6 (Figure 4.4, Table 4.5). However, a two-parameter linear correlation using the electronic parameter σ and steric parameter V_W shows a lower χ^2 value than the single-parameter correlation with just V_W (Table 4.5). The ρ value is more negative at pH 8.6 by 0.5 as compared with pH 6.6, whereas the coefficient for V_W is essentially unaffected by pH (Table 4.5).

Analyses of the effects the substituents of N,N'-(4-X-benzyl)$_2$-1,4-diaminobutanes have on the steady-state kinetic parameters k_{cat}/K_M and k_{cat} are summarized in Table 4.6. The best linear correlation for k_{cat}/K_M is obtained with the

single-parameter π giving a coefficient of 1.03 ± 0.27, though the χ^2 value for this fit is only 0.35. Two-parameter correlations did not result in improved fits. These poor correlations can be attributed to the low K_M values with these substrates (Table 4.1). With k_{cat}, the best linear correlation is with the two-parameter fit consisting of V_W and σ. This is the same result as observed with k_{red}, and the ρ value for k_{cat} of -0.34 ± 0.13 (Table 4.6) is close to the ρ value of -0.59 ± 0.04 for k_{red} (Table 4.5).

Table 4.5: Correlation analysis of log k_{red} for N,N'-(4-X-benzyl)$_2$-1,4-diaminobutanes with hydrophobic, steric and electronic parameters.

	pH 6.6		pH 8.6	
Parameter	**Coefficient**	χ^2	**Coefficient**	χ^2
σ	-0.45 ± 0.30	0.53	-1.02 ± 0.36	0.77
σ^+	-0.31 ± 0.16	0.43	-0.64 ± 0.17	0.53
σ^-	-0.14 ± 0.50	0.75	-0.69 ± 0.76	1.69
σ_I	0.23 ± 0.86	0.75	-0.37 ± 1.38	1.94
π	-0.05 ± 0.40	0.76	-0.42 ± 0.62	1.80
V_W	0.39 ± 0.03	0.02	0.58 ± 0.12	0.32
E_S	-0.20 ± 0.13	0.23	-0.13 ± 0.20	0.52
V_W *	0.36 ± 0.02	0.00881	0.40 ± 0.04	0.02
σ^+ *	-0.06 ± 0.03		-0.37 ± 0.04	
V_W *	0.37 ± 0.02	0.00869	0.45 ± 0.02	0.01
σ *	-0.09 ± 0.05		-0.59 ± 0.04	

* Fits for single-parameter linear correlations were done using eq 4.7, and two-parameter linear correlations were done using eq 4.8.

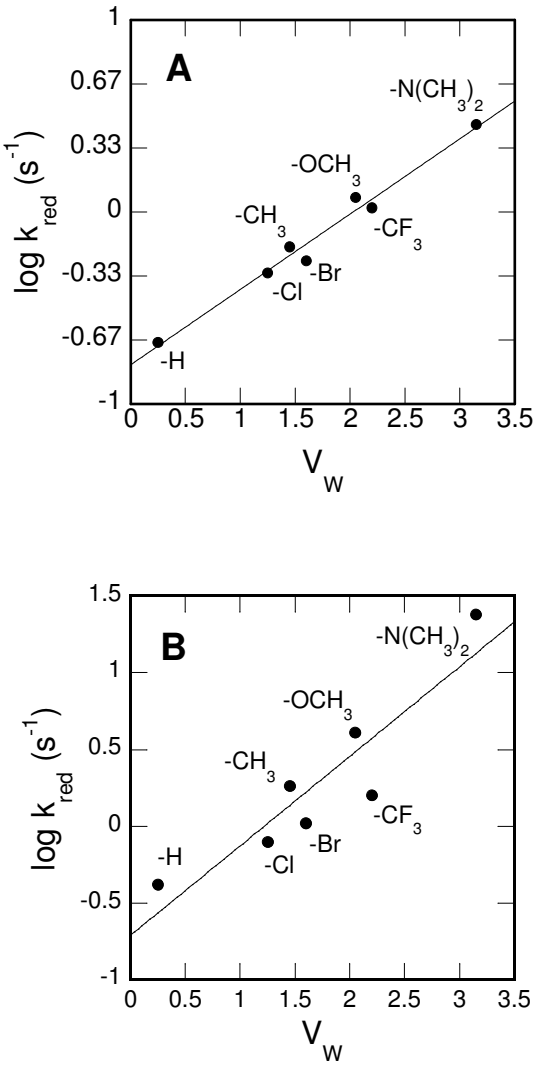

Figure 4.4: Correlation of the k_{red} values for para-substituted N,N'-(4-X -benzyl)$_2$-1,4-diaminobutanes as substrates for PAO with the van der Waals volume (V_W) of the substituents at (A) pH 6.6 and (B) pH 8.6. The lines are from fits to a single-parameter linear correlation with the steric parameter V_w shown in eq 4.7.

Table 4.6: Correlation analysis of log k_{cat}/K_M (μM^{-1} s^{-1}) and log k_{cat} (s^{-1}) with N,N'-(4-X-benzyl)$_2$-1,4-diaminobutanes at 30 °C with hydrophobic, steric and electronic parameters at pH 8.6.

	k_{cat}/K_M (μM^{-1} s^{-1})		k_{cat} (s^{-1})	
Parameter	**Coefficient**	χ^2	**Coefficient**	χ^2
σ	0.63 ± 0.39	0.87	-0.61 ± 0.24	0.36
σ^+	0.31 ± 0.23	1	0.39 ± 0.13	0.28
σ^-	0.76 ± 0.58	0.99	-0.49 ± 0.47	0.65
σ_I	2.00 ± 0.71	0.52	-0.32 ± 0.87	0.78
π	1.03 ± 0.27	0.35	-0.20 ± 0.40	0.76
V_W	0.06 ± 0.23	1.3	0.36 ± 0.08	0.17
E_S	-0.35 ± 0.18	0.71	-0.11 ± 0.16	0.35
V_W	0.32 ± 0.23	0.68	0.26 ± 0.08	0.07
σ^+	0.52 ± 0.27		0.21 ± 0.09	
V_W	0.23 ± 0.20	0.63	0.28 ± 0.06	0.06
σ	0.86 ± 0.41		-0.34 ± 0.13	

** Fits for single-parameter linear correlations were done using eq 4.7, and two-parameter linear correlations were done using eq 4.8.

DISCUSSION

These studies with N,N'-(4-X-benzyl)$_2$-1,4-diaminobutane present the opportunity to address the minimal substrate required for PAO recognition. Specifically, the ability of PAO to oxidize N,N'-(4-X-benzyl)$_2$-1,4-diaminobutane indicates that PAO requires two nitrogens separated by four carbons, and hence the diaminobutane core with the appropriate protonation state is what is important for binding and catalysis. Previous studies of PAO with the natural substrates N1-acetylspermine and N1-acetylspermidine are consistent with the nitrogen at the site of CH bond cleavage being neutral and one other nitrogen being positively charged in the reactive form of the substrate (Chapter II). The k_{cat}/K_M-pH profiles described here are consistent with earlier observations using the natural substrates, that the monoprotonated form of N,N'-(4-X-benzyl)$_2$-1,4-diaminobutane is the active form of the substrate. Studies of PAO with N1,N12-bisethylspermine (BESPM) and N1,N11-bis(ethyl)-nor-spermine (BENSPM) reveal that PAO also recognizes them as substrates and catalyzes their oxidation (*26, 79*). BESPM and BENSPM, like the N,N'-(4-X-benzyl)$_2$-1,4-diaminobutanes, contain the diaminobutane core that exists in the appropriate protonation state for catalysis. However, spermidine and N8-acetylspermidine, are competitive inhibitors (*26*) despite containing the diaminobutane core. In comparing the structures of these polyamines, it appears as though having the diaminobutane core is the minimal substrate requirement for substrate recognition, but that length and volume play an important role in orienting the substrate in a manner compatible for catalysis.

The transient kinetic studies indicate that the rate constant k_{red} is slightly lower than k_{cat} for the N,N'-(4-X-benzyl)$_2$-1,4-diaminobutanes. One explanation for the lower k_{red} is that the enzyme is slightly less active at higher enzyme concentrations. The similar k_{red} and k_{cat} values establish that reduction is the rate-limiting step in catalysis (Table 4.1). Furthermore, the spectral changes observed for all seven N,N'-(4-X-benzyl)$_2$-1,4-diaminobutanes establish that flavin reduction occurs in a single step, with no observation of any intermediates. N,N'-(4-X-Benzyl)$_2$-1,4-diaminobutanes are slow substrates in which chemistry is the rate-limiting step, thus allowing for the build-up of intermediates if such intermediates exist. The rate constant associated with flavin reduction for N1-acetylspermine is over 1000-fold greater (Chapter II) than those observed with N,N'-(4-X-benzyl)$_2$-1,4-diaminobutanes. The k_{red}-pH profiles observed for N1-acetylspermine displays a decrease in activity at acidic pH with a pK_a of 7.3 ± 0.1, consistent with the ability of substrate in the incorrectly protonated form to bind to the enzyme, but not react. The k_{red}-pH profile for N,N'-(4-H-benzyl)$_2$-1,4-diaminobutane is a sigmoid curve, indicating that both the protonated and deprotonated forms of the enzyme-substrate complex are active, but deprotonation enhances activity or that the proton can be lost from the ES complex at a rate of ~0.2 s^{-1}. The change in activity between the protonated and deprotonated forms is only ~4-fold. Coupled with the fact that the isotope effect on k_{red} is pH-independent, this suggests that the deprotonation that enhances the rate of reduction is a local perturbation that does not affect the chemistry step. It is feasible that the proton is lost to solvent since it is unlikely a base exists in the active site to accept the proton. Previous studies of K315M PAO show that this Lys315

does not behave as an active site base, and furthermore does not play a role in flavin reduction (Chapter II). Thus, the loss of a proton to solvent seems the most likely explanation. With natural substrates that display a rate constant for flavin reduction that is significantly faster, the rate constant of 0.20 s^{-1} associated with the loss of a proton during the transition-state is not observed, indicating that this deprotonation is not significant for catalysis with physiological substrates. A source of this deprotonation could be explained by the presence of water molecules that can pack inside the active site with the N,N'-(4-X-benzyl)$_2$-1,4-diaminobutane substrates that are not present in the active site with N1-acetylspermine bound.

The isotope effects on k_{cat}/K_{DBDB} and k_{cat} for N,N'-(4-X -benzyl)$_2$-1,4-diaminobutanes in Table 3 are less than two for the three substrates analyzed and are pH-independent, indicating that this may be the intrinsic effect. Similar pH-dependent isotope effects on k_{red} (Table 4.4) are observed in the oxidation of N,N'-(4-X-benzyl)$_2$-1,4-diaminobutanes by PAO, indicating that there are no external commitments. These results cumulatively indicate that CH bond cleavage is the rate-limiting step in reduction. The small magnitude of the isotope effects can be indicative of either an internal commitment or a very early transition state. Similar small isotope effects have been seen with other flavoprotein amine oxidases including LSD1 (Chapter VI), DAAO (*98*), and TMO (*99*).

Analysis of single- and two-parameter linear correlations of k_{red} with electronic (σ, $\sigma+$, and $\sigma-$), hydrophobic (π), and steric (V_W and E_S) parameters at the pH optimum of 8.6 and at pH 6.6 allows for assessment of the charge development during the

transition state. Two-parameter linear correlations with V_W and σ show the best fits. At both pH 6.6 and 8.6, the coefficient associated with V_W is pH-independent, whereas the electronic parameter coefficient approaches zero away from the pH optimum. Going from the pH optimum of 8.6 to the pH value of 6.6 results in an increase in the ρ value from -0.59 to -0.09; thus, the effect of the substrate amine pK_a could be to make the ρ value more positive at low pH by ~0.5. Therefore, it is likely that the pH-dependence of the correlation observed with k_{red} and the σ factor at high pH but not a low pH is due to the pK_a of N,N'-(4-X-benzyl)$_2$-1,4-diaminobutanes in the ES complex and not charge development in the transition state. Another explanation could be the loss of a proton at a rate of 0.2 s^{-1} that results from additional water molecules hydrogen-bonded within the active site of PAO with N,N'-(4-X-benzyl)$_2$-1,4-diaminobutane substrates.

These results with PAO are consistent with studies of oxidation of *para*-substituted benzylamine analogues by MAO-B, where a correlation between k_{red} the Taft steric parameter indicating that steric orientation of the substrate is important for flavin reduction (*46*). However, with monoamine oxidase A (*45*), Miller and Edmondson report a positive correlation for k_{red} and the electronic parameter σ with a ρ value of 1.8 ± 0.3. The reason for the differences in the ρ value observed for MAO-A versus MAO-B is not clear, especially in light of the fact that MAO-A and MAO-B are 70% identical. Furthermore, results from structure-activity relationships with MAO-A in the oxidation of phenethylamine analogues show that the k_{red} value decreases with an increase in the V_W parameter of the substituent in a linear manner and that binding affinities of a series of arylalkylamine analogues have the best linear correlation with the Taft steric

parameter of the alkyl side chain (*100*). No electronic contribution was observed. A difference between the linear correlations with electronic parameters in the oxidation of benzylamine and phenethylamine analogues is expected. The presence of the extra CH_2 group in phenethylamine would cause a 2-3 fold reduction in the ρ value (*101*). However, a significant ρ value is still expected. A possible explanation for the linear correlations with the electronic parameter σ observed for MAO-A with *para*-substituted benzylamine analogues is that the source of the linear correlation is due to the pK_a of the benzylamine substrates, rather than the charge development of ES complex in the transition state, as is observed with PAO. This is a likely explanation since amine substrates are able to ionize at the pH value studied, and thus can contribute to correlations with electronic parameters. As with PAO, the ρ value increases going above the pK_a, -0.59 to -0.09, so the argument that the ρ value may be pH sensitive and the experiment should be done in the pH-insensitive region is valid.

The mechanism of flavin amine oxidases has been a source of debate for years with three prominant mechanisms at the center of the controversy including single electron transfer, polar nucleophilic addition, and hydride transfer mechanisms. The single electron transfer mechanism proposed by Silverman involves the formation of a radical intermediate of the flavin or a residue within the enzyme's active site (Figure 1.8) (*39*). The polar nucleophilic mechanism as put forth by Edmondson is a concerted reaction involving the formation of a 4a-alkylated isoalloxazine ring that activates the N5 of the flavin for proton abstraction of the substrate α-hydrogen (Figure 1.9) (*45*). The hydride transfer mechanism is the simplest mechanism, involving the direct transfer

of a hydride from the α-C of the substrate to the N5 position of the flavin (Figure 1.10). This last mechanism has received greater attention for the MAO/PAO family only in recent years (*47, 49-51, 97*) despite the fact that it is and has been the accepted mechanism for D-amino acid oxidase (*48, 66*).

A large amount of data has been generated in recent years concerning flavoprotein amine oxidases. To date, no flavin intermediates have been observed, which supports the hydride transfer mechanism. ^{15}N kinetic isotope effects for N-methyltryptophan oxidase (*51*), TMO (*49*), and DAAO (*48*) rule out the polar nucleophilic mechanism. The small ρ value presented here for PAO with N'-(4-X-benzyl)$_2$-1,4-diaminobutanes indicates a lack of charge development in the transition state, consistent with hydride transfer. Interpretation of all this data in terms of the three potential mechanisms proposed for flavoprotein amine oxidases provides an overwhelming amount of evidence in favor of the hydride transfer mechanism.

CHAPTER V

USE OF pH AND KINETIC ISOTOPE EFFECTS TO ESTABLISH CHEMISTRY AS RATE-LIMITING IN OXIDATION OF A PEPTIDE SUBSTRATE BY LSD1*

Nucleosomes, the basic subunits of chromatin, are composed of 146 bp of DNA wrapped around an octamer of four core histones (H3, H4, H2A and H2B) (*102*). Each octamer consists of an H3-H4 histone tetramer plus an H2A-H2B dimer and is connected to the adjacent octamers via an H1 linker histone (*102*). Post-translational modifications of the N-terminal tails of histones, which extend freely beyond the nucleosome core, have been shown to affect chromatin structure and the accessibility to DNA of proteins essential for transcription, repair, and replication (*103*). Lysine-specific demethylase (LSD1) is an FAD-containing amine oxidase that catalyzes the demethylation of mono- and dimethylated lysyl residues in the N-terminal tails of histones, thereby playing a role in the epigenetic regulation of gene transcription in cells (*76*). LSD1 demethylates lysine residues 4 and 9 of histone H3 (H3K4 and H3K9) (*104, 105*); in addition, the enzyme can demethylate the tumor suppressor p53 (*106*). The discoveries of LSD1 and of the JmjC family of iron(II)-alpha-ketoglutarate-dependent histone demethylases (*107*) have demonstrated that methylation of histones is not permanent; instead, like other post-translational modifications, it is part of a reversible process. The effects of histone methylation vary depending on the site of modification, the degree of methylation, the

---

* Reproduced with permission from Gaweska, H., Henderson Pozzi, M., Schmidt, D. M. Z., McCafferty, D. G., and Fitzpatrick, P.F. (2009) *Biochemistry 48*, 5440-5445.

sites and nature of adjacent modifications, and the protein complexes in proximity to the modification (*108*). LSD1 functions as both a repressor and activator of gene transcription; for example, demethylation of Lys4 of histone H3 results in gene repression (*109*), while androgen-dependent demethylation of mono- or dimethylated Lys9 results in an activated transcriptional state (*105*). LSD1 has been implicated in the maintenance of disease, such as neuroblastoma (*110*), its expression correlates with high-risk prostate tumors (*111*), and it plays regulatory roles in cell differentiation (*112, 113*).

Flavoprotein oxidases utilize a flavin cofactor to catalyze oxidation of a substrate CX bond, transferring a hydride equivalent to the flavin; the reduced flavin is then oxidized by molecular oxygen, producing H_2O_2 (*114*). LSD1 oxidizes the carbon-nitrogen bond between the methyl group and the epsilon amine of lysyl residues, forming an imine intermediate that is nonenzymatically hydrolyzed to produce formaldehyde and the demethylated lysine (Figure 5.1). There are two structural families of flavoprotein amine oxidases; LSD1 belongs to the monoamine oxidase family (*32*). A number of mechanisms have been proposed for amine oxidation by flavoenzymes, including direct transfer of a hydride transfer from the substrate to the flavin, formation of a substrate carbanion that then transfers electrons to the flavin, and two single electron transfers to form an intermediate radical pair with a subsequent proton transfer (*65*). However, kinetic isotope effects on the reactions of a number of flavoprotein amine and alcohol oxidases support direct hydride transfer as the mechanism for members of both families of amine oxidases and for flavoprotein oxidases in general (*48, 49, 51, 66, 115*).

While there have been many studies focusing on the role of LSD1 in gene transcription and protein expression and its interactions with other proteins, few have focused on the kinetics of the enzyme. Several mechanism-based inhibitors of monoamine oxidase and their derivatives have been shown to inhibit LSD1 (*109, 116-120*), providing insights into the interactions with substrates and demonstrating the mechanistic similarity of the enzyme to monoamine oxidase. Forneris et al. have described a pH profile of LSD1 (*121*) and analyzed the reaction of the photo-reduced enzyme with oxygen, demonstrating that the oxidation is typical of a flavoprotein oxidase (*122*). Still, there has been no detailed analysis of the reaction with a normal peptide substrate that allows for conclusions regarding mechanism. LSD1 is highly specific for the N-terminus of histone H3. Indeed, the minimal substrate is a peptide composed of the N-terminal 21 amino acid residues of H3 (*121*). We describe here mechanistic studies of oxidation of such a peptide substrate by LSD1.

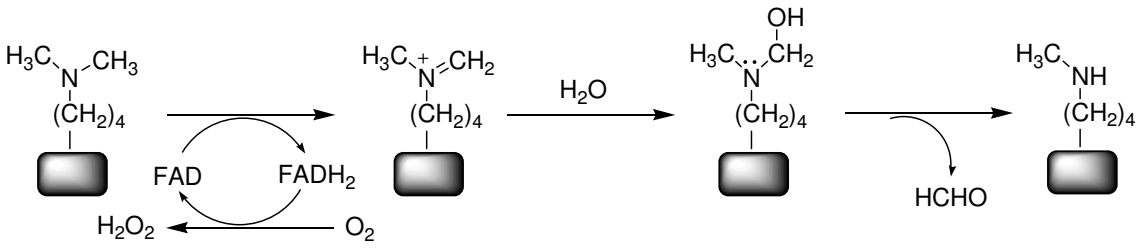

Figure 5.1: LSD1 oxidation of lysine in histone3.

EXPERIMENTAL PROCEDURES

Materials. Horseradish peroxidase and Ampliflu Red were purchased from Sigma. Fmoc amino acids were from Novabiochem, Applied Biosystems, or Advanced ChemTech. ^{2}H-Formaldehyde (20% solution in D_2O) was from Cambridge Isotopes. Sodium cyanoborodeuteride was from CDN Isotopes.

H3K4 21-mer Dimethylated Peptide Synthesis. A peptide corresponding to the first 21 amino acids of histone H3 with a dimethylated lysine at the fourth residue (ARTK(diMe)QTARKSTGGKAPRKQLA) was synthesized by Helena Gaweska of Duke University (*123*). Similarly, the deuterated dimethylated H3K4 peptide was also synthesized by Helena Gaweska.

LSD1 Expression and Purification. A truncated form of human LSD1, lacking the first 150 amino acids (*76*), was expressed and purified by Helena Gaweska of Duke University (*123*). The concentration of LSD1 was determined using the absorbance at 458 nm and an extinction coefficient based on that for free FAD (11,600 $cm^{-1}M^{-1}$).

Assays. Steady state kinetic assays monitoring oxygen consumption were performed on a computer-interfaced Hansatech (Hansatech Instruments) or YSI (Yellow Springs Instrument, Inc.) oxygen electrode. All assays were conducted at 25 °C and were initiated by the addition of enzyme. A fluorescence assay, coupling hydrogen peroxide formation to oxidation of Ampliflu Red by horseradish peroxidase, was used to determine k_{cat}/K_m values due to the low concentrations of substrate required. The product resorufin was detected using a fluorescence plate reader (Molecular Devices SpectraMax Gemini EM) with an excitation wavelength of 560 nm and emission at 590

nm. Experiments done using the fluorescence assay were conducted by Helena Gaweska of Duke University. The coupled fluorescence assay resulted in initial rates that were twofold slower than those detected using the oxygen electrode. Consequently, the rates obtained with the coupled assay were corrected by this factor. The constant ionic strength buffer 0.1 M Aces, 52 mM Tris, and 52 mM ethanolamine (*124*) was used for assays at all pH values. Preincubation of enzyme in buffers of pH higher than 9.5 for 60 minutes eliminated LSD1 activity.

Rapid-reaction kinetic experiments were conducted at 25 ºC on an Applied Photophysics SX-18MV stopped-flow spectrophotometer. Anaerobic conditions were established by applying cycles of vacuum and argon to enzyme solutions, while substrate solutions were bubbled with argon. The buffer was again ACES/Tris/ethanolamine, plus 5 mM glucose, at pH 7.5. Glucose oxidase was added to all anaerobic solutions at a final concentration of 36 nM before loading them onto the stopped-flow spectrophotometer.

Data Analysis. Steady-state kinetic data were analyzed using the program KaleidaGraph (Adelbeck Software, Reading, PA). Initial rate data obtained by varying the concentration of a single substrate were fit to the Michaelis-Menten equation. The effects of pH on kinetic parameters were fit to eq 5.1, which applies for a kinetic parameter which decreases below pK_1 due to protonation of a single moiety and decreases above pK_2 due to deprotonation of a single moiety. Here, y is the kinetic parameter being measured, c is its pH-independent value, and K_1 and K_2 are the ionization constants for moieties which must be unprotonated or protonated, respectively. Eq 5.2 was used to determine kinetic isotope effects using the program Igor

(WaveMetrics, Lake Oswego, OR); *E* is the isotope effect on the parameters $k_{cat}/K_{21\text{-}mer}$ and k_{cat}, S is the concentration of H3K4 21-mer dimethylated peptide, and F_i is the fraction of heavy atom in the substrate. Analysis of stopped-flow data was done using both KaleidaGraph and SPECFIT (Spectrum Software Associates, Marlborough, MA). To determine the kinetic parameters for the reduction of LSD1, stopped-flow traces were fit to eq 5.3, which describes a monophasic exponential decay; k_1 is the first order rate constant, A_1 is the total absorbance change, and A_∞ is the final absorbance.

$$\log y = \log (c/(1 + H/K_1 + K_2/H)) \quad (5.1)$$

$$v = (k_{cat}*S)/((K_M + S)*(1 + (E - 1)*F_i) \quad (5.2)$$

$$A_t = A_1 e^{-k_1 t} + A_\infty \quad (5.3)$$

RESULTS

Steady-State Kinetics. Steady-state kinetic parameters for LSD1 were determined at pH 7.5 and 25 °C with the dimethylated H3K4 21-mer as substrate. This peptide has the sequence of the N-terminal 21 residues of histone H3, the physiological substrate of LSD1, and contains N, N-dimethyllysine at residue 4. It represents the minimum length required for detectable activity (*121*). While the $k_{cat}/K_{21\text{-}mer}$ values could be determined in air-saturated buffer because LSD1 exhibits ping pong kinetics (*122*), k_{cat} values were determined with 1.1 mM oxygen and 50 μM peptide to ensure saturation with both substrates. In addition, the k_{cat}/K_{O2} values were determined by varying the concentration of oxygen in the presence of 50 μM peptide. The results are summarized in Table 1. The k_{cat} and $k_{cat}/K_{21\text{-}mer}$ values are in reasonable agreement with the values previously reported by Forneris et al. (*121*).

pH Profiles. The effect of pH on the $k_{cat}/K_{21\text{-}mer}$ values was determined over the pH range 7.0–9.5 using a buffer system that maintained constant ionic strength over the entire pH range. At pH values above 9.5, the enzyme lost activity, while the activity was too low below pH 7 to be measured reliably. Because these assays are not carried out with saturating oxygen concentrations, the resulting k_{cat} values were only apparent, and the k_{cat}-pH profile need not reflect the actual pK_a values. The $k_{cat}/K_{21\text{-}mer}$ data yield a bell-shaped pH profile (Figure 5.2), decreasing above and below pH 8.5-9. This behavior is consistent with the involvement of two groups on the free enzyme or substrate, one of which must be protonated and one deprotonated for activity. When the data were fit assuming different pK_a values for the two groups, the resulting pK_a values were within

0.3 of one another (results not shown), too close to reliably discriminate. Consequently, only the average of the pK_a values of the two groups can be determined. The data were therefore fit using eq 5.1, which assigns the same pK_a value to the two groups, to obtain the average pK_a value of 8.7 ± 0.1.

Kinetic Isotope Effects Deuterium kinetic isotope effects were determined with the 21-mer in which both methyl groups on the dimethylated lysyl residue contained three deuteriums. The results at pH 7.5 are summarized in Table 5.1. Data obtained by varying the concentration of the peptide in air-saturated buffer were best fit by eq 5.2, which assigns equal values to $^{D}k_{cat}/K_{21\text{-}mer}$ and $^{D}k_{cat}$, for an isotope effect of 3.2 ± 0.1. Alternatively, the $^{D}k_{cat}$ value was determined at fixed saturating concentrations of peptide and oxygen of 50 μM and 1.1 mM, respectively. The resulting value was 2.9 ± 0.2. The kinetic isotope effect on $k_{cat}/K_{21\text{-}mer}$ and k_{cat} was then determined over the pH range 7-9.5, fitting the data in each case to eq 5.2. The isotope effect was pH-independent, with an average value of 3.5 ± 0.3 (Table 5.2). The effect of pH on the $k_{cat}/K_{21\text{-}mer}$ value for the deuterated peptide is shown in Figure 5.2; these data were fit to eq 5.1 to yield an average pK_a value of 8.8 ± 0.1, within error of the value for the nondeuterated peptide.

Table 5.1: Kinetic parameters of LSD1 with the H3K4 21-mer dimethylated peptide as a substrate∗

Kinetic parameter	Value
$k_{cat}/K_{21\text{-}mer}$ (mM^{-1} s^{-1})	38 ± 2[a]
k_{cat}/K_{O2} (mM^{-1} s^{-1})	1.0 ± 0.2[b]
$K_{21\text{-}mer}$ (μM)	2.6 ± 0.2[a]
K_{O2} (μM)	195 ± 40[b]
k_{cat} (s^{-1})	0.199 ± 0.013[c]
k_{red} (s^{-1})	0.231 ± 0.004[e]
$^{D}(k_{cat}/K_{21\text{-}mer})$	3.2 ± 0.1[a,d]
$^{D}k_{cat}$	2.9 ± 0.2[c] 3.2 ± 0.1[a,d]
$^{D}k_{red}$	3.3 ± 0.1[e]

∗Conditions: pH 7.5, 25 °C.
[a]Determined in air-saturated buffer.
[b]Determined using 50 μM H3K4 21-mer dimethylated peptide.
[c]Determined using 50 μM H3K4 21-mer dimethylated peptide and 1.1 mM oxygen.
[d]Calculated using eq 5.2.
[e]Determined using 200 μM 21-mer dimethylated peptide.

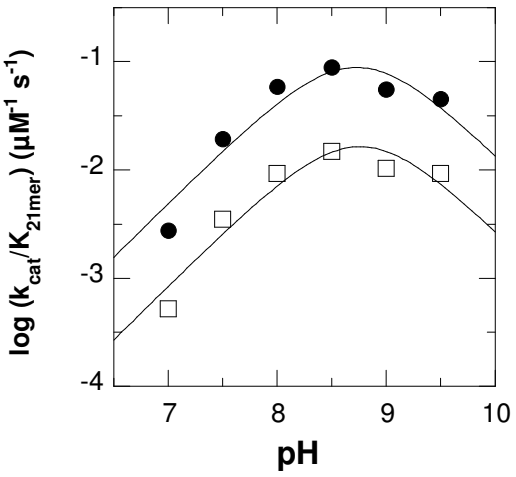

Figure 5.2: k_{cat}/K_M pH profiles for LSD1 with protiated (closed circles) and deuterated (open squares) H3K4 21-mer dimethylated peptide. The lines are from fits of the data to eq 5.1.

Table 5.2: Effect of pH on the deuterium kinetic isotope effects on the oxidation of the H3K4 21-mer dimethylated peptide by LSD1*

pH	Kinetic isotope effect
7.0	4.0 ± 0.2
7.5	3.2 ± 0.1
8.0	3.3 ± 0.1
8.5	3.4 ± 0.1
9.0	3.7 ± 0.2
9.5	3.6 ± 0.1
Average	3.5 ± 0.3

*Determined in air saturated buffers and calculated using eq 5.2.

Flavin Reduction Kinetics. Stopped-flow spectroscopy was used to study reduction of the flavin in LSD1 by saturating concentrations (200 μM) of the 21-mer at pH 7.5. The changes in the absorbance of the enzyme-bound flavin after mixing LSD1 anaerobically with the 21-mer are best fit as a single exponential decay (Figure 5.3). The rate constant for reduction (k_{red}) with this substrate concentration is within error of the k_{cat} value (Table 5.1), consistent with reduction being rate-limiting for turnover. The k_{red} value was also determined with 200 μM deuterated peptide, yielding a $^{D}k_{red}$ value of 3.3 ± 0.1. This value is identical to the pH-independent isotope effect determined in the steady-state kinetic analyses. To more definitively confirm that reduction consists of a single kinetic phase, the reaction was repeated using a photodiode array detector to monitor the flavin spectrum from 325 to 600 nm. Over this wavelength range, there is no evidence for an intermediate between oxidized flavin and reduced flavin (Figure 5.3B). A global analysis of the spectral changes during flavin reduction as a single exponential decay allowed the spectra of the starting and final enzyme to be determined (Figure 5.3C). These confirm that the oxidized and reduced enzyme are the only species that can be detected.

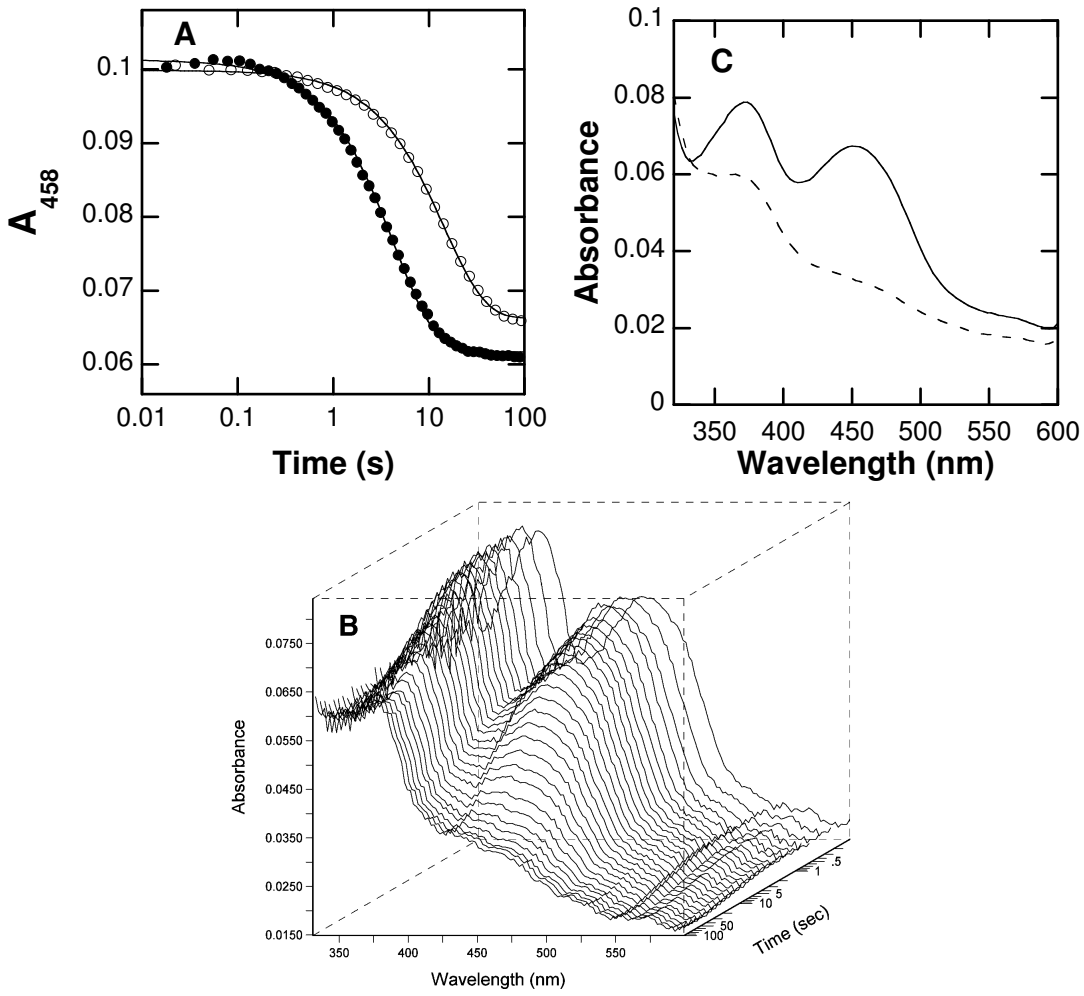

Figure 5.3: Spectral changes during reduction of LSD1 by the H3K4 21-mer dimethylated peptide. A, time course at 458 nm with protiated (closed circles) or deuterated (open circles) substrate (only 1/30th of the points are shown for clarity); B, Changes in the entire visible absorbance spectrum during reduction by the deuterated substrate; C, Initial (—) and final (···) spectra upon LSD1 flavin reduction by deuterated H3K4 21-mer dimethyl peptide obtained from a global analysis of the data in B using a single-step kinetic model. The lines in A are from fits of the data to eq 5.3.

DISCUSSION

While the physiological substrate for LSD1 is the histone H3, mechanistic studies with the entire protein substrate present significant problems, including the difficulty of preparing the dimethylated substrate. Consequently, mechanistic insight requires the use of a minimal substrate which still retains the specificity determinants of the larger protein. LSD1 has no detectable activity with peptides containing fewer than 16 of the N-terminal residues of histone H3, and a peptide containing the first 21 residues, as was utilized here, is as active a substrate as a peptide containing the first 30 residues (*121*). Epigenetic modifications of histone H3 that alter the reactivity of the intact protein with LSD1 cause similar decreases in activity when incorporated into a 21-mer (*122*), establishing the latter as a valid model for the larger protein substrate. Indeed, incorporation of a propargyl moiety onto Lys4 of the 21-mer yields an efficient mechanism-based inhibitor (*116*). The three-dimensional structure of the inactivated enzyme shows extensive contacts with the first 7 residues, while the remainder of the peptide is not visible (*118*). This combination of solution and structural studies establishes the validity of the 21-mer as a model for mechanistic studies.

The steady-state and transient kinetic studies presented here establish that the rate-limiting step in oxidation of the dimethylated H3K4 21-mer by LSD1 is CH bond cleavage. The k_{red} value, the rate constant for flavin reduction, is identical to the k_{cat} value for LSD1. Therefore, the reductive half reaction is rate-limiting for turnover with this peptide substrate. The identity of the primary deuterium isotope effects on $k_{cat}/K_{21\text{-}mer}$, k_{cat}, and k_{red} further identifies CH bond cleavage as the rate limiting step. The pH-

independence of the isotope effect on $k_{cat}/K_{21\text{-mer}}$ is also consistent with fully rate-limiting CH bond cleavage and suggests that this isotope effect is the intrinsic deuterium isotope effect (*125*). An isotope effect of 3.2 ± 0.1 is substantially smaller than the limiting semi-classical value of about 7 for a primary deuterium isotope effect (*126*); in the present case, the value also includes the secondary isotope effects from the two other deuterium atoms on each methyl group. The small magnitude of the isotope effect suggests that the oxidation of this substrate by LSD1 has an early transition state. A late transition state would also yield a small isotope effect, but a late transition state would be expected for an unfavorable reaction. In contrast, at all concentrations of substrate used here, the reductive half-reaction goes to completion rather than reaching an equilibrium suggesting that the oxidation of the 21-mer is favorable. Similarly small kinetic isotope effects have been reported for other flavin amine oxidases, including **D**-amino acid oxidase with glycine as substrate (*98*) and tryptophan 2-monooxygenase with tryptophan as substrate (*99*).

No intermediates between oxidized and reduced enzyme were observed in the oxidation of the 21-mer by LSD1. The lack of an intermediate with a substrate whose rate-limiting step is CH bond cleavage is not consistent with several mechanisms proposed for flavin amine oxidases, especially mechanisms involving easily detectable flavin radicals or covalent substrate-flavin adducts. The present results are fully consistent with direct hydride transfer as the mechanism of LSD1, in line with observations from other flavoprotein amine oxidases. LSD1 is inactivated by cyclopropyl substrates (*120*), and inactivation by such compounds is frequently taken as

evidence for radical intermediates (*39*). However, a number of flavoprotein oxidases for which hydride transfer is the accepted mechanism can be inactivated by cyclopropyl substrates (*42, 127*).

The kinetic parameter $k_{cat}/K_{21\text{-}mer}$ exhibits a pH optimum of 8.7 in the studies described here. While the k_{cat}/K_m value for a substrate can reflect the protonation states of both the enzyme and substrate required for productive binding and catalysis, recent studies with the related flavoprotein polyamine oxidase suggest that the k_{cat}/K_m-pH profile reflects the required protonation state of the substrate. With N1-acetylspermine, N1-acetylspermidine, and spermine as the substrate for mammalian polyamine oxidase, the k_{cat}/K_{amine}-pH optimum matches the pH at which the substrate has only one positively charged nitrogen (Chapter II). The pH dependence of the inhibition by spermidine analogues further established that the nitrogen in the CN bond of the polyamine being oxidized by polyamine oxidase must be uncharged for oxidation, consistent with observations of other amine oxidases (*48-50*) and with the expectations for a hydride transfer mechanism. With both polyamine oxidase (Chapter II) and monoamine oxidase (*83*), the need for the nitrogen at the reaction site to be neutral is clearly seen in the pH dependence of the reductive half reaction of the enzyme, demonstrating the requirement for a neutral nitrogen for catalysis. The substrate used in the present study contains the first 21 residues of the N-terminus of histone H3. Based on the precedents of other amine oxidases, the dimethylated Lys4 must be uncharged for catalysis and therefore is responsible for the acidic limb of the pH profile. Protonation of Lys4 does not prevent binding since the trimethylated analog of this peptide binds tightly

to LSD1, although it is not a substrate (*121*). The basic limb of the $k_{cat}/K_{21\text{-}mer}$-pH profile can be attributed to one of the three other lysyl residues in the substrate.

The members of the monoamine oxidase family, including LSD1, contain a conserved lysyl residue in the active site that is part of a "Lys-H_2O-N5" structural motif (*32, 34, 73-76*). This residue clearly could be a source of a pK_a in the $k_{cat}/K_{21\text{-}mer}$-pH profile. Mutation of this lysine in LSD1 to an alanine results in a complete loss of activity (*87*), and in maize polyamine oxidase the corresponding lysine to methionine mutation results in a 1400-fold decrease in k_{red} (*59*). However, the same lysine to methionine mutation in mouse polyamine oxidase results in no change in the k_{cat}/K_{amine}-pH profile and only a slight decrease in the value of k_{red} (Chapter II), suggesting that this residue plays a subtle structural rather than a catalytic role in these enzymes and therefore does not contribute to the pH dependence.

The rate constant for the chemical step in LSD1 is 2-5 orders of magnitude slower than values reported for other flavoprotein amine oxidases (*46, 59, 86, 128-130*). This suggests that evolution has not optimized catalysis for this enzyme. Instead, it is likely that the requirements for rapid catalysis are secondary to high specificity in this case. Given the physiological role of LSD1 in regulation of gene expression, high catalytic activity would be much less critical than very high specificity. Moreover, while high catalytic activity is necessary for metabolic enzymes to maintain balance among metabolic pathways, epigenetic regulation such as DNA histone methylation operates on a very long time scale and would not require rate constants on the order of 10^2-10^4 s^{-1}.

CHAPTER VI

SUMMARY

The purpose of this study is to determine the chemical mechanism by which mammalian polyamine oxidase (PAO) catalyzes the oxidation of polyamines. PAO catalyzes the oxidation of N1-acetylspermine and N1-acetylspermidine to produce N-acetyl-3-aminopropanaldehyde and spermidine or putrescine. Structurally, PAO is a member of the monoamine oxidase family of flavoproteins. The three mechanisms proposed for flavin amine oxidases are a single electron transfer mechanism producing a radical intermediate, a polar nucleophilic mechanism forming a covalent adduct intermediate, and a direct hydride transfer.

The effects of pH on kinetic parameters for mouse PAO were determined to gain insight into the protonation state of the polyamine required for catalysis and the roles of ionizable residues in the active site in amine oxidation. The k_{cat}/K_{amine}-pH profiles are bell-shaped for N1-acetylspermine, N1-acetylspermidine, and spermine, with each of the profiles being consistent with the productive form of the substrate possessing a single positively charged nitrogen. The pK_i-pH profiles for a series of polyamine analogs are most consistent with the reactive form of the substrate having a neutral nitrogen at the site of oxidation and one positively charged nitrogen. With N1-acetylspermine as the substrate, the value of the limiting rate constant for flavin reduction, k_{red}, is pH dependent, decreasing below a pK_a value of 7.3, offering further validation for the requirement of an uncharged nitrogen for substrate oxidation. In PAO, Lys315

corresponds to a conserved active site residue found throughout the monoamine oxidase family. Mutating of Lys315 to methionine does not affect the k_{cat}/K_{amine} profile for spermine, the k_{red} value with N1-acetylspermine is only decreased by 1.8-fold compared to wild-type enzyme, and the pK_a of the k_{red}-pH profile with N1-acetylspermine shows a basic shift to 7.8. These results rule out Lys315 as a source of a pK_a in the k_{cat}/K_{amine} or k_{cat}/k_{red} profiles and establish that this residue does not play a critical role in amine oxidation by PAO.

Steady-state kinetic parameters and the pH-dependence of k_{cat}/K_{O2} for wild-type and K315M PAO establish that Lys315 plays a role in the oxidative half-reaction. A 30-fold decrease in k_{cat}/K_{O2} is observed for the mutant enzyme. The k_{cat}/K_{O2}-pH profiles for wild-type and K315M PAO indicate that the unprotonated form of Lys315 is required for optimal catalysis. Solvent isotope effects and proton inventories of wild-type and K315M PAO suggest that the absence of this lysyl residue can be overcome by replacement with a water molecule. The "Lys-H_2O-N5" structural motif identified in members of the MAO structural family, in PAO must involve a hydrogen-bond network between unprotonated Lys315 and the active site water molecule. Thus it is conceivable that Lys315 enhances the rate of oxidation of reduced flavin by facilitating the removal of the proton from the N5 position of reduced FAD.

The influence that substituents in the aromatic ring of N,N'-(4-X-benzyl)$_2$-1,4-diaminobutanes have on steady-state kinetic parameters and the k_{red} value for PAO is the focus of Chapter IV. The k_{cat}/K_M-pH profiles for N, N'-dibenzyl-1,4-diaminobutane and the CH_3O- and CF_3-substituted compounds all show a bell-shaped curve, consistent with

the monoprotonated form of the substrate being required for binding and catalysis. The rate constants of flavin reduction are >1000-fold slower than those observed for natural substrates, and kinetics with all analogues reveal that the rate-limiting step in turnover is flavin reduction. The k_{red}-pH profile displays a sigmoidal shape, with a pK_a of 8.2 ± 0.3. Isotope effects on k_{cat}, k_{cat}/K_M, and k_{red}, are pH-independent, with an average value of 2, indicating an internal commitment or an early transition state. The k_{red} values for N,N'-(4-X-benzyl)$_2$-1,4-diaminobutanes exhibit a correlation with the van der Waals volume (V_W) of the substituent that is pH independent, and with the σ parameter. The ρ value is -0.059 at pH 8.6, and -0.09 at pH 6.6. The change in the ρ value as a function of pH can be attributed to changes in pK_a of the N,N'-(4-X-benzyl)$_2$-1,4-diaminobutane substrates in the ES complex. The data presented here are best interpreted as further support for the hydride transfer mechanism.

The mechanism of oxidation of a peptide substrate by the flavoprotein lysine-specific demethylase (LSD1) was examined using the effects of pH and isotopic substitution on steady-state and rapid-reaction kinetic parameters as presented in Chapter V. The peptide substrate is composed of the first 21 residues of the N-terminal tail of histone H3, with a dimethylated lysyl residue at position 4. At pH 7.5, k_{red} equals k_{cat}, indicating that the reductive half reaction is rate-limiting at physiological pH. Deuteration of the lysyl methyls results in identical kinetic isotope effects of 3.1 ± 0.2 on the k_{red}, k_{cat} and k_{cat}/K_m values for the peptide, establishing CH bond cleavage as rate-limiting with this substrate. No intermediates between oxidized and reduced flavin are detectable by stopped-flow spectroscopy, consistent with the expectation for a direct

hydride transfer mechanism. The k_{cat}/K_m pH-profile for the peptide is bell-shaped, consistent with a requirement that the nitrogen at the site of oxidation be uncharged and that at least one of the other lysyl residues be charged for catalysis. The $^{D}(k_{cat}/K_m)$ value for the peptide is pH-independent, suggesting that the observed value is the intrinsic deuterium kinetic isotope effect for oxidation of this substrate.

REFERENCES

(1) van Leeuwenhoek, A. (1678) Observations D. Anthonii Leeuwenhoek, de Natis e semine genitali Animalculis. *Philos. Trans. R. Soc. London 12*, 1040-1043.

(2) Dudley, H. W., Rosenheim, M.C., and Rosenheim, O. (1924) The chemical constitution of spermine. 1. The isolation of spermine from animal tissues and the preparation of its salts. *Biochem. J. 18*, 1263-1272.

(3) Matthews, H. R. (1993) Polyamine, chromatin structure and transcription. *BioEssays 15*, 561-567.

(4) Tabor, C. W., and Tabor, H. (1984) Polyamines. *Annu. Rev. Biochem. 53*, 749-790.

(5) Xaio, L., Swank, R.A., and Matthews, H.R. (1991) Photoaffinity polyamines: Sequence specific interactions with DNA. *Nucleic Acid Res. 19*, 3701-3708.

(6) Basu, H. S., Wright, W. D., Deen, D. F., Roti-Roti, J., and Marton, L. J. (1993) Treatment with a polyamine analogue alters DNA matrix association in HeLa cell nuclei: A nucleoid halo assay. *Biochemistry 32*, 4073-4076.

(7) Morgan, J. E., Blankenship, J. W., and Matthews, H. R. (1987) Polyamines and acetylpolyamines increase the stability and alter the conformation of nucleosome core particles. *Biochemistry 26*, 3643-3649.

(8) Wallace, H. M., Fraser, A. V., and Hughes, A. (2003) A perspective of polyamine metabolism. *Biochem. J. 376*, 1-14.

(9) Wallace, H. M. (1996) Polyamines in human health. *Proc. Nutr. Soc. 55*, 419-431.

(10) Soulet, D., Gagnon, B., Rivest, S., Audette, M., and Poulin, R. (2004) A fluorescent probe of polyamine transport accumulates into intracellular acidic vesicles via a two-step mechanism. *J. Biol. Chem. 279*, 49355-49366.

(11) Belting, M., Mani, K., Jonsson, M., Cheng, F., Sandgren, S., Jonsson, S., Ding, K., Delcros, J.G., and Fransson, L.A. (2003) Glypican-1 is a vehicle for polyamine uptake in mammalian cells. *J. Biol. Chem. 278*, 47181-47189.

(12) Seiler, N., Delcros, J.G., and Moulinoux, J.P. (1996) Polyamine transport in mammalian cells. *An update. Int. J. Biochem. Cell. Biol. 28*, 843-861.

(13) Bolkenius, F. N., and Seiler, N. (1981) Acetyl derivatives as intermediates in polyamine catabolism. *Int. J. Biochem. 13*, 287-292.

(14) Kingsnorth, A. N., and Wallace, H. M. (1985) Elevation of monoacetylated polyamines in human breast cancers. *J. Cancer Clin. Oncol. 21*, 1057-1062.

(15) Wallace, H. M., Duthie, J., Evans, D.M., Lamond, S., Nicoll, K.M., and Heys, S.D. (2000) Alterations in polyamine catabolic enzymes in human breast cancer tissue. *Clin. Cancer Res. 6*, 3657-3661.

(16) Parchment, R. E., and Pierce, G. B. (1989) Polyamine oxidation, programmed cell death, and regulation of melanoma in the murine embryonic limb. *Cancer Res. 49*, 6680-6686.

(17) Averill-Bates, D. A., Agostinelli, E., Przybytkowski, E. and Mondovi, B. (1994) Aldehyde dehydrogenase and cytotoxicity of purified bovine serum amine

oxidase and spermine in Chinese hamster ovary cells. *Biochem. Cell Biol. 72*, 36-42.

(18) Wallace, H. M., and Fraser, A.V. (2004) Inhibitors of polyamine metabolism: Review article. *Amino Acids 26*, 353-365.

(19) Gerner, E. W. a. M., P.S. (1986) Restoration of polyamine contents in rat hepatoma (HTC) cells after inhibition of polyamine biosynthesis: Relationship with cell proliferation. *Eur. J. Biochem. 156*, 31-35.

(20) Byers, T. L., Ganem, B., and Pegg, A.E. (1992) Cytostasis induced in L1210 murine leukaemia cells by the S-adenosyl-L-methionine decarboxylase inhibitor 5'([(Z)-4-amino-2-butenyl]methylamino)-5'-deoxyadenosine may be due to hypusine depletion. *Biochem. J. 287*, 717-724.

(21) Pegg, A. E. (1986) Recent advances in the biochemistry of polyamines in eukaryotes. *Biochem. J. 234*, 249-262.

(22) Karvonen, E., Kauppinen, L., Partanen, T., and Poso, H. (1985) Irreversible inhibition of putrescine-stimulated S-adenosyl-L-methionine decarboxylase by berenil and pentamidine. *Biochem. J. 231*, 165-169.

(23) Wolff, A. C., Armstrong, D.K., Fetting, J.H., Carducci, M.K., Riley, C.D., Bender, J.F., Casero, Jr, R.A., and Davidson, N.E. (2003) A Phase II study of the polyamine analog N1,N11-diethylnorspermine (DENSpm) daily for five days every 21 days in patients with previously treated metastatic breast cancer. *Clin. Cancer Res. 9*, 5922-5928.

(24) Lin, P. K. T., Dance, A.M., Bestwick, C., and Milne, L. (2003) The biological activities of new polyamine derivatives as potential therapeutic agents. *Biochem. Soc. Trans. 31*, 407-410.

(25) Ha, H. C., Woster, P.M., Yager, J.D, and Casero, Jr., R.A. (1997) The role of polyamine catabolism in polyamine analogue-induced programmed cell death. *Proc. Natl. Acad. Sci. U.S.A. 94*, 11557-11562.

(26) Wu, T., Yankovskaya, V., and McIntire, W. S. (2003) Cloning, sequencing, and heterologous expression of the murine peroxisomal flavoprotein, N1-acetylated polyamine oxidase. *J. Biol. Chem. 278*, 20514-20525.

(27) Houen, G., Bock, K., and Jensen, A.L. (1994) HPLC and NMR investigation of the serum amine oxidase catalyzed oxidation of polyamines. *Acta. Chem. Scand. 48*, 52-60.

(28) Vujcic, S., Liang, P., Diegelman, P., Kramer, D. L., and Porter, C. W. (2003) Genomic identification and biochemical characterization of the mammalian polyamine oxidase involved in polyamine back-conversion. *Biochem. J. 370*, 19-28.

(29) Silverman, R. B. (2002) *The organic chemistry of enzyme-catalyzed reactions*, Elsevier Sciences, San Diego, California.

(30) Gadda, G., and Fitzpatrick, P.F. (1998) Biochemical and physical characterization of the active FAD-containing form of nitroalkane oxidase from *Fusarium oxysprum*. *Biochemistry 37*, 6154-6164.

(31) Kearney, E. B., Salach, J.I., Walker, W.H., Seng, R.L., Kenney, W., Zeszotek, E., and Singer, T.P. (1971) The covalently-bound flavin of hepatic monoamine oxidase. 1. Isolation and sequence of a flavin peptide and evidence for binding at the 8alpha position. *Eur. J. Biochem. 24*, 321-327.

(32) Chen, Y., Yang, Y., Wang, F., Wan, K., Yamane, K., Zhang, Y., and Lei, M. (2006) Crystal structure of human histone lysine-specific demethylase 1 (LSD1). *Proc. Natl. Acad. Sci. U.S.A. 103*, 13956-13961.

(33) Landry, J., and Sternglanz, R. (2003) Yeast Fms1 is a FAD-utilizing polyamine oxidase. *Biochem. Biophys. Res. Commun. 303*, 771-776.

(34) Pawelek, P. D., Cheah, J., Coulombe, R., Macheroux, P., Ghisla, S., and Vrielink, A. (2000) The structure of L-amino acid oxidase reveals the substrate trajectory into a enantiomerically conserved active site. *EMBO J. 19*, 429404215.

(35) Sobrado, P., and Fitzpatrick, P.F. (2003) Analysis of the role of the active site residue Arg98 in the flavoprotein tryptophan 2-monooxygenase, a member of the L-amino oxidase family. *Biochemistry 42*, 13826-13832.

(36) Knoll, J. (1992) Pharmacological basis of the therapeutic effect of (-)deprenyl in age-related neurological diseases. *Med. Res. Rev. 12*, 505-524.

(37) Rinne, U. (1987) R-(-)-deprenyl as an adjuvant to levodopa in the treatment of Parkinson's disease. *J. Neural. Transm. 25 Suppl*, 149-155.

(38) Edmondson, D. E., Mattevi, A., Binda, C., Li, M., and Hubalek, F. (2004) Structure and mechanism of monoamine oxidase. *Curr. Med. Chem. 11*, 1983-1993.

(39) Silverman, R. B. (1995) Radical ideas about monoamine oxidase. *Acc. Chem. Res. 28*, 335-342.

(40) Newton-Vinson, P., and Edmondson, D. E. (1999) High-level expression, structural, kinetic and redox characterization of recombinant human liver monoamine oxidase B., in *Flavins and Flavoproteins* (Ghisla, S., Kroneck, P., Macheroux, P., and Sund, H., Ed.) pp 431, Agency for Scientific Publications, Berlin.

(41) Sherry, B., and Abeles, R.H. (1985) Mechanism of action of methanol oxidase, reconstitution of methanol oxidase with 5-deazaflavin, and inactivation of methanol oxidase by cyclopropanol. *Biochemistry 24*, 2594-2605.

(42) McCann, A. E., and Sampson N.S. (2002) A C6-flavin adduct Is the major product of irreversible inactivation of cholesterol oxidase by 2α,3α-cyclopropano-5α-cholestan-3β-ol. *J. Am. Chem. Soc. 122*, 35-39.

(43) Hamilton, G. A. (1971) Proton in biological redox reactions. *Prog. Bioorg. Chem. 1*, 83-157.

(44) Edmondson, D. E., Binda, C., Mattevi, A. (2007) Structural insights into the mechanism of amine oxidation by monoamine oxidases A and B. *Arch. Biochem. Biophys. 264*, 269-276.

(45) Miller, J. R., and Edmondson, D. E. (1999) Structure-activity relationships in the oxidation of *para*-substituted benzylamine analogues by recombinant human liver monoamine oxidase A. *Biochemistry 38*, 13670-13683.

(46) Walker, M. C., and Edmondson, D.E. (1994) Structure-activity relationships in the oxidation of benzylamine analogues by bovine liver mitochondrial monoamine oxidase B. *Biochemistry 33*, 7088-7098.

(47) Denu, J. M., and Fitzpatrick, P. F. (1994) Intrinsic primary, secondary, and solvent kinetic isotope effects on the reductive half-reaction of D-amino acid oxidase: evidence against a concerted mechanism. *Biochemistry 33*, 4001-4007.

(48) Kurtz, K. A., and Fitzpatrick, P.F. (2000) Nitrogen isotope effects as probes of the mechanism of D-amino acid oxidase. *J. Am. Chem. Soc 122*, 12896-12897.

(49) Ralph, E. C., Anderson, M. A., Cleland, W. W., and Fitzpatrick, P. F. (2006) Mechanistic studies of the flavoenzyme tryptophan 2-monooxygenase: Deuterium and ^{15}N kinetic isotope effects on alanine oxidation by an L-amino acid oxidase. *Biochemistry 45*, 15844-15852.

(50) Ralph, E. C., and Fitzpatrick, P. F. (2005) pH and kinetic isotope effects on sarcosine oxidation by *N*-methyltryptophan oxidase. *Biochemistry 44*, 3074-3081.

(51) Ralph, E. C., Hirschi, J. S., Anderson, M. A., Cleland, W. W., Singleton, D. A., and Fitzpatrick, P. F. (2007) Insights into the mechanism of the flavoprotein-catalyzed amine oxidation from nitrogen isotope effects of the reaction of *N*-methyltryptophan oxidase. *Biochemistry 46*, 7655-7664.

(52) Mattevi, A., Vanoni, M.A., Todone, F., Rizzi, M., Teplyakov, A., Coda, A., Bolognesi, M., and Curti, B. (1996) Crystal Structure of D-amino acid oxidase: A

case of active site mirror-image convergent evolution with flavocytochrome b_2. *Proc. Natl. Acad. Sci. U.S.A. 93*, 7496-7501.

(53) Sobrado, P., and Fitzpatrick, P.F. (2002) Analysis of the roles of amino acid residues in the flavoprotein tryptophan 2-monooxygenase modified by 2-oxo-3-pentynoate: Characterization of His338, Cys339, and Cys511 mutant enzymes. *Arch. Biochem. Biophys. 402*, 24-30.

(54) Marton, L. J., and Pegg, A.E. (1995) Polyamines as targets for therapeutic intervention. *Annu. Rev. Pharmacol. Toxicol. 35*, 55-91.

(55) Wang, Y., and Casero, R.A., Jr. (2006) Mammalian polyamine catabolism: a therapeutic target, a pathological problem, or both? *J. Biochem. (Tokyo) 139*, 17-25.

(56) Vujcic, S., Diegelman, P., Bacchi, C.J., Kramer, D.L., and Porter, C.W. (2002) Identification and characterization of a novel flavin-containing spermine oxidase of mammalian cell origin. *Biochem. J. 367*, 665-667.

(57) Wang, Y., Murray-Stewert, T., Devereux, W., Hacker, A., Frydman, B., Woster, P.M. and Casero, R.A., Jr. (2003) Properties of purified recombinant human polyamine oxidase, PAOh1/SMO. *Biochem. Biophys. Res. Commun. 304*.

(58) Cervelli, M., Polticelli, F., Federico, R., and Mariottini, P. (2003) Heterologous expression and characterization of mouse spermine oxidase. *J. Biol. Chem. 278*, 5271-5276.

(59) Polticelli, F., Basran, J., Faso, C., Cona, A., Minervini, G., Angeline, R., Federico, R., Scrutton, N. S., and Tavladoraki, P. (2005) Lys300 plays a major

role in the catalytic mechanism of polyamine oxidase. *Biochemistry 44*, 16108-16120.

(60) Binda, C., Mattevi, A., and Edmondson, D. E. (2002) Structure-function relationships in flavoenzyme-dependent amine oxidases. *J. Biol. Chem. 277*, 23973-23976.

(61) Binda, C., Angelini, R., Federico, R., Ascenzi, P., and Mattevi, A. (2001) Structural bases for inhibitor binding and catalysis in polyamine oxidase. *Biochemistry 40*, 2766-2776.

(62) Bellelli, A., Angelini, R., Laurenzi, M., and Federico, R. (1997) Transient kinetics of polyamine oxidase from Zea mays L. *Arch. Biochem. Biophys. 343*, 146-148.

(63) Sebela, M., Radova, A., Angelini, R., Tavladoraki, P., Frebort, I.I., and Pec, P. (2001) FAD-containing polyamine oxidases: A timely challenge for researchers in biochemistry and physiology of plants. *Plant Sci. 160*, 197-207.

(64) Bright, H. J., and Porter, D.J.T. (1975) Flavoprotein oxidases, in *The Enzymes* (Boyer, P., Ed.) pp 421-505, Academic Press, New York.

(65) Fitzpatrick, P. F. (2001) Substrate dehydrogenation by flavoproteins. *Acc. Chem. Res. 42*, 299-307.

(66) Fitzpatrick, P. F. (2007) Insights into the mechanisms of flavoprotein oxidases from kinetic isotope efects. *J. Label Compd. Radiopharm. 50*, 1016-1025.

(67) Scrutton, N. S. (2004) Chemical aspects of amine oxidation by flavoprotein enzymes. *Nat. Prod. Rep. 21*, 722-730.

(68) Zhao, G., and Jorns, M.S. (2006) Spectral and kinetic characterization of the Michaelis charge transfer complex in monomeric sarcosine oxidase. *Biochemistry 45*, 5985-5992.

(69) Harris, C. M., Pollegioni, L., and Ghisla, S. (2001) pH and kinetic isotope effects in D-amino acid oxidase catalysis. *Eur. J. Biochem. 268*, 5504-5520.

(70) Zhao, G., Song, H., Chen, Z., Mathews, S., and Jorns, M.S. (2002) Monomeric sarcosine oxidase: Role of histidine 269 in catalysis. *Biochemistry 41*, 9751-9764.

(71) Jones, T. Z., Balsa, D., Unzeta, M., and Ramsay, R.R. (2007) Variations in activity and inhibition with pH: The protonated amine is the substrate for monoamine oxidase, but uncharged inhibitors bind better. *J. Neural Transm. 113*, 707-712.

(72) Trickey, P., Wagner, M.A., Jorns, M.S., and Mathews, F.S. (1999) Monomeric sarcosine oxidase: Role of histidine 269 in catalysis. *Structure 7*, 331-345.

(73) Binda, C., Coda, C., Angelini, R., Ascenzi, P., and Mattevi, A. (1999) A 30-Å long U-shaped catalytic tunnel in the crystal structure of polyamine oxidase. *Structure 7*, 265-276.

(74) Huang, Q., Liu, Q., and Hao, Q. (2005) Crystal structures of Fms1 and its complex with spermine reveal substrate specficity. *J. Mol. Biol. 348*, 951-959.

(75) Binda, C., Newton-Vinson, P., Hubalek, F., Edmondson, D.E., and Mattevi, A. (2002) Structure of human monoamine oxidase B, a drug target for the treatment of neurological disorders. *Nat. Struct. Biol. 9*, 22-26.

(76) Ma, J., Yoshimura, M., Yamashita, E., Nakagawa, A., Ito, A., and Tsukihara, T. (2004) Structure of rat monoamine oxidase A and its specific recognitions for substrates and inhibitors. *J. Mol. Biol. 338*, 103-114.

(77) Gawandi, V., and Fitzpatrick, P.F. (2007) The synthesis of deuterium-labeled spermine, N1-acetylspermine and N1-acetylspermidine. *J. Label Compd. Radiopharm. 50*, 666-670.

(78) Henderson Pozzi, M., Gawandi, V., and Fitzpatrick, P.F. (2009) pH Dependence of a mammalian polyamine oxidase: Insights into substrate specificity and the role of lysine 315. *Biochemistry 48*, 1508-1516.

(79) Royo, M., and Fitzpatrick, P.F. (2005) Mechanistic studies of mouse polyamine oxidase with N1,N12-bisethylspermine as a substrate. *Biochemistry 44*, 7079-7084.

(80) Frassineti, C., Ghelli, S., Gans, P., Sabatini, A., Moruzzi, M.S., and Vacca, A. (1995) Nuclear magnetic resonance as a tool for determining protonation constants of natural polyprotic bases in solution. *Anal. Biochem. 231*, 374-382.

(81) Bencini, A., Bianchi, A., Garcia-Espana, E., Micheloni, M., and Remirez, J.A. (1999) Proton coordination by polyamine compounds in aqueous solution. *Coord. Chem. Rev. 188*, 97-156.

(82) Zhao, G., and Jorns, M.S. (2005) Ionization of zwitterionic amine substrates bound to monomeric sarcosine oxidase. *Biochemistry 44*, 16866-16874.

(83) Dunn, R. V., Marshall, K.R., Munro, A.W., and Scrutton, N.S. (2008) The pH dependence of kinetic isotope effects in monoamine oxidase A indicates

stabilization of the neutral amine in the enzyme-substrate complex. *FEBS Journal 275*, 3850-3858.

(84) Dansen, T. B., Wirtz, K.W.A., Wanders, R.J.A., and Pap, E.H.W. (1999) Peroxisomes in human fibroblasts have a basic pH. *Nat. Cell Biol. 2*, 51-53.

(85) Ghisla, S., and Massey, V. (1991) L-Lactate Oxidase, in *Chemistry and Biochemistry of Flavoenzymes, Vol. II* (Muller, F., Ed.) pp 243-289, CRC Press, Boca Raton.

(86) Emanuele, J. J., and Fitzpatrick, P.F. (1995) Mechanistic studies of the flavoprotein tryptophan 2-monooxygenase. 1. Kinetic mechanism. *Biochemistry 34*, 3710-3715.

(87) Lee, M. G., Wynder, C., Cooch, N., and Shiekhattar, R. (2005) An essential role for CoREST in nucleosomal histone 3 lysine 4 demethylation. *Nature 437*, 432-435.

(88) Segur, J. B., and Oberstar, H.E. (1951) Viscosity of glycerol and Its aqueous solutions. *Ind. Eng. Chem. 43*, 2117-2120.

(89) Roth, J. P., and Klinman, J.P. (2002) Catalysis of electron transfer during activation of O_2 by the flavoprotein glucose oxidase. *Proc. Natl. Acad. Sci. U.S.A. 100*, 62-67.

(90) Rungsrisuriyachai, K., and Gadda, G. (2008) On the role of histidine 351 in the reaction of alcohol oxidation by choline oxidase. *Biochemistry 47*, 6762-6769.

(91) Ghanem, M., and Gadda, G. (2005) On the catalytic role of the conserved active site residue His_{466} of choline oxidase. *Biochemistry 44*, 893-904.

(92) Seiler, N. (1987) Functions of polyamine acetylation. *Can. J. Physiol. Phatmacol. 65*, 2024-2035.

(93) Thomas, T., and Thomas, T. J. (2003) Polyamine metabolism and cancer. *J. Cell Mol. Med. 7*, 113-126.

(94) Wang, Y., Devereux, W., Woster, P.M., Stewart, T.M., Hacker, A., and Casero, R.A. Jr. (2001) Cloning and characterization of a human polyamine oxidase that is inducible by polyamine analogue exposure. *Cancer Res. 61*, 5370-5373.

(95) Casero, R. A., Jr., Wang, Y., Stewart, T.M., Devereux, W., Hacker, A., Wang, Y., Smith, R., and Woster, P.M. (2003) The role of polyamine catabolism in anti-tumour drug response. *Biochem. Soc. Trans. 31*, 361-365.

(96) Pollegioni, L., Blodig, W., and Ghisla, S. (1997) On the mechanism of D-amino acid oxidase. *J. Biol. Chem. 272*, 4924-4934.

(97) Fitzpatrick, P. F. (2004) Carbanion versus hydride transfer mechanisms in flavoprotein-catalyzed dehydrogenations. *Bioorg. Chem. 32*, 125-139.

(98) Denu, J. M., and Fitzpatrick, P. F. (1992) pH and kinetic isotope effects on the reductive half-reaction of D-amino acid oxidase. *Biochemistry 31*, 8207-8215.

(99) Emanuele, J. J., and Fitzpatrick, P.F. (1995) Mechansitic studies of the flavoprotein tryptophan 2-monooxygenase. 2. pH and kinetic isotope effects. *Biochemistry 34*, 3716-3723.

(100) Nandigama, R. K., and Edmondson, D.E. (2000) Structure-activity relations in the oxidation of phenethylamine analogues by recombinant human liver monoamine oxidase A. *Biochemistry 39*, 15258-15265.

(101) Taft, J., R.W., and Lewis, I.C. (1959) Evaluation of resonance effects on reactivity by application of the linear inductive energy relationship. V. Concerning a σ_R scale of resonance effects. *J. Am. Chem. Soc. 81*, 5343-5352.

(102) Luger, K., Mader, A.W., Richmond, R.K., Sargent, D.F., and Richmond, T.J. (1997) Crystal structure of the nucleosome core particle at 2.8 Å resolution. *Nature 389*, 251-260.

(103) Jenuwein, T., and Allis, C.D. (2001) Translating the histone code. *Science 293*, 1074-1080.

(104) Shi, Y., Lan, F., Matson, C., Mulligan, P., Whetsine, J.R., Cole, P.A., and Casero, R.A. (2004) Histone demethylation mediated by the nuclear amine oxidase homolog LSD1. *Cell. Mol. Life Sci. 119*, 941-953.

(105) Metzger, E., Wissmann, M., Yin, N., Muller, J.M., Schneider, R., Peters, A.H.F.M., Gunther, T., Buettner, R., and Schule, R. (2005) LSD1 demethylates repressive histone marks to promote androgen-receptor-dependent transcription. *Nature 437*, 436-439.

(106) Huang, J., Sengupta, R., Espejo, A.B., Lee, M.G., Dorsey, J.A., Richter, M., Opravil, S., Shiekhattar, R., Bedford, M.T., Jenuwein, T., and Berger, S.L. (2007) p53 is regulated by the lysine demethylase LSD1. *Nature 449*, 105-108.

(107) Tsukada, Y., Fang, J., Erdjument-Bromage, H., Warren, M.E., Borchers, C.H., Tempst, P., and Zhang, Y. (2006) Histone demethylation by a family of JmjC domain-containing proteins. *Nature 439*, 811-816.

(108) Shilatifard, A. (2008) Molecular implementation and physiological roles for histone H3 lysine 4 (H3K4) methylation. *Curr. Opin. Cell Biol. 20*, 341-348.

(109) Lee, M. G., Wynder, C., Schmidt, D.M., McCafferty, D.G., and Shiekhattar, R. (2006) Histone H3 Lysine 4 demethylation is a target of nonselective antidepressive medications. *Chem. Biol. 13*, 563-567.

(110) Schulte, J. H., Lim, S., Schramm, A., Friedrichs, N., Koster, J., Versteeg, R., Ora, I., Pajtler, K., Klein-Hitpass, L., Kuhfittig-Kulle, S., Metzger, E., Schule, R., Eggert, A., Buettner, R., and Kirfel, J. (2009) Lysine-specific demethylase 1 is strongly expressed in poorly differentiated neuroblastoma: Implications for therapy. *Cancer Res. 69*, 2065-2071.

(111) Kahl, P., Gullotti, L., Heukamp, L.C., Wolf, S., Friedrichs, N., Vorreuther, R., Solleder, G., Bastian, P.J., Ellinger, J., Metzger, E., Schule, R., and Buettner, R. (2006) Androgen receptor coactivators lysine-specific histone demethylase 1 and four and a half LIM domain protein 2 predict risk of prostate cancer recurrence. *Cancer Res. 66*, 11341-11347.

(112) Zhu, X., Wang, J., Ju, B.G., and Rosenfeld, M.G. (2007) Signaling and epigenetic regulation of pituitary development. *Curr. Opin. Cell Biol. 19*, 605-611.

(113) Su, S. T., Ying, H.Y., Chiu, Y.K., Lin, F.R., Chen, M.Y., and Lin, K.I. (2009) Involvement of histone demethylase LSD1 in Blimp1-mediated gene repression during plasma cell differentiation. *Mol. Cell. Biol. 29*, 1421-1431.

(114) Fraaije, M. W., and Mattevi, A. (2000) Flavoenzymes: Diverse catalysts with recurrent features. *Trends Biochem. Sci. 25*, 126-132.

(115) Sobrado, P., and Fitzpatrick, P.F. (2003) Solvent and primary deuterium isotope effects show that lactate CH and OH bond cleavages are concerted in Y254F flavocytochrome b_2, consistent with a hydride transfer mechanism. *Biochemistry 42*, 15208-15214.

(116) Culhane, J. C., Szewczuk, L.M., Liu, X., Da, G., Marmorstein, R., and Cole, P.A. (2006) A mechanism-based inactivator for histone demethylase LSD1. *J. Am. Chem. Soc. 128*, 4536-4537.

(117) Szewczuk, L. M., Culhane, J.C., Yang, M., Majumdar, A., Yu, H., and Cole, P.A. (2007) Mechanistic analysis of a suicide inactivator of histone demethylase LSD1. *Biochemistry 46*, 6892-6902.

(118) Yang, M., Culhane, J.C., Szewczuk, L.M., Jalili, P., Ball, H.L., Machius, M., Cole, P.A., and Yu, H. (2007) Structural basis for the inhibition of the LSD1 by the antidepressant trans-2-phenylcyclopropylamine. *Biochemistry 46*, 8058-8065.

(119) Gooden, D. M., Schmidt, D.M.Z., Pollock, J.A., Kabadi, A.M., and McCafferty, D.G. (2008) Facile synthesis of substituted trans-2-arylcyclopropylamine inhibitors of the human histone demethylase LSD1 and monoamine oxidases A and B. *Bioorg. Med. Chem. Lett. 18*, 3047-3051.

(120) Schmidt, D. M., and McCafferty, D. G. (2007) *trans*-2-Phenylcyclopropylamine in a mechanism-based inactivator of the histone demethylase LSD1. *Biochem. 46*, 4408-4416.

(121) Forneris, F., Binda, C., Vanoni, M.A., Battaglioli, E., and Mattvie, A. (2005) Human histone demethylase LSD1 reads the histone code. *J. Biol. Chem. 280*, 41360-41365.

(122) Forneris, F., Binda, C., Dall'Aglio, A., Fraaije, M.W., Battaglioli, E., and Mattevi, A. (2006) A highly specific mechanism of histone H3-K4 recognition by histone demethylase LSD1. *J. Biol. Chem. 281*, 35289-35295.

(123) Gaweska, H., Henderson Pozzi, M., Schmidt, D. M. Z., McCafferty, D. G., and Fitzpatrick, P.F. (2009) Use of pH and kinetic isotope effects to establish chemistry as rate-limiting in oxidation of a peptide substrate by LSD1. *Biochemistry 48*, 5440-5445.

(124) Ellis, K. J., and Morrison, J.F. (1982) Buffers of constant ionic strength for studying pH-dependent processes. *Methods Enzymol. 87*, 405-426.

(125) Cook, P. F., and Cleland, W.W. (1981) pH variation of isotope effects in enzyme-catalyzed reactions. 1. Isotope- and pH-dependent steps the same. *Biochemistry 20*, 1797-1805.

(126) Jencks, W. P. (1969) *Catalysis in chemistry and enzymology*, McGraw-Hill Books, Inc, New York.

(127) Chen, Z. W., Zhao, G., Martinovic, S., Jorns, M.S., and Mathews, F.S. (2005) Structure of the sodium borohydride-reduced N-(cyclopropyl)glycine adduct of the flavoenzyme monomeric sarcosine oxidase. *Biochemistry 44*, 15444-15450.

(128) Massey, V., and Gibson, Q.H. (1964) Role of semiquinones in flavoprotein catalysis. *Fed. Proc. 23*, 18-29.

(129) Massey, V., and Curti, R. (1967) On the reaction mechanism of *Crotalus adamanteus* L-amino acid oxidase. *J. Biol. Chem. 242*, 1259-1264.

(130) Basran, J., Bhanji, N., Basran, A., Nietlispach, D., Mistry, S., Meskys, R., and Scrutton, N.S. (2002) Mechanistic aspects of the covalent flavoprotein dimethylglycine oxidase of *Arthrobacter globiformis* studied by stopped-flow spectrophotometry. *Biochemistry 41*, 4733-4743.

VITA

Michelle Henderson Pozzi
TAMU Dept of Biochemistry
103 Biochemistry Bldg
2128 TAMU
College Station, TX 77843-2128
shp3@tamu.edu

Education
B.S., Chemistry, Sam Houston State University, 2004
Ph. D., Texas A&M University, 2010

Honors and Awards

2000-01	Alpha Lambda Delta-National Academic Freshman Honor Society, Texas Lutheran University
2000-02	Pace-Setters Scholarship, Texas Lutheran University
	Provost List, Texas Lutheran University
2002-03	Undergraduate Academic Achievement Scholarship, Sam Houston State University
	Deans List, Sam Houston State University
	National Deans List
2002-04	Earl H. Burrough Endowed Scholarship, Sam Houston State University
	Deans List, Sam Houston State University
	Alpha Chi Academic Honor Society, Sam Houston State University
	Beta Beta Beta National Biological Honor Society, Sam Houston State University
2004	Graduated summa cum laude, Sam Houston State University
2004-06	NIH Molecular Biophysics Trainee, Texas A&M University

Publications

Gaweska, H., **Henderson Pozzi, M.**, Schmidt, D.M.Z., McCafferty, and Fitzpatrick, P.F. (2009) Use of pH and Kinetic Isotope Effects to Establish Chemistry as Rate-Limiting in Oxidation of Peptide Substrate. *Biochemistry 48*, 5440-5445.

Henderson Pozzi, M., Gawandi, V., and Fitzpatrick, P.F. (2009) pH-Dependence of a Mammalian Polyamine Oxidase: Insights into Substrate Specificity and the Role of Lysine 315. *Biochemistry 48*, 1508-1516.

Livingston, A.L., Kundu, S., **Henderson Pozzi, M.**, Anderson, D.W., and David, S.S. (2005) Insights into the Roles of Tyrosine 82 and Glycine 253 in the *Escherichia coli* Adenine Glycosylase MutY. *Biochemistry 44*, 14179-14190.